

Fixed-Weight Difference Target Propagation

Tatsukichi Shibuya,¹ Nakamasa Inoue,¹ Rei Kawakami,¹ Ikuro Sato^{1,2}

¹ Tokyo Institute of Technology

² Denso IT Laboratory

shibuya.t.ad@m.titech.ac.jp, inoue@c.titech.ac.jp, reikawa@sc.e.titech.ac.jp, isato@c.titech.ac.jp

Abstract

Target Propagation (TP) is a biologically more plausible algorithm than the error backpropagation (BP) to train deep networks, and improving practicality of TP is an open issue. TP methods require the feedforward and feedback networks to form layer-wise autoencoders for propagating the target values generated at the output layer. However, this causes certain drawbacks; *e.g.*, careful hyperparameter tuning is required to synchronize the feedforward and feedback training, and frequent updates of the feedback path are usually required than that of the feedforward path. Learning of the feedforward and feedback networks is sufficient to make TP methods capable of training, but is having these layer-wise autoencoders a necessary condition for TP to work? We answer this question by presenting *Fixed-Weight Difference Target Propagation* (FW-DTP) that keeps the feedback weights constant during training. We confirmed that this simple method, which naturally resolves the abovementioned problems of TP, can still deliver informative target values to hidden layers for a given task; indeed, FW-DTP consistently achieves higher test performance than a baseline, the Difference Target Propagation (DTP), on four classification datasets. We also present a novel propagation architecture that explains the exact form of the feedback function of DTP to analyze FW-DTP.

1 Introduction

Artificial Neural Networks (NNs) were introduced to model the information processing in the neural circuits of the brain (McCulloch and Pitts 1943; Rosenblatt 1958). The error backpropagation (BP) has been the most widely used algorithm to optimize parameters of multi-layer NNs with gradient descent (Rumelhart, Hinton, and Williams 1986), but the lack of consistency with neuroscientific findings has been pointed out (Crick 1989; Glorot and Bengio 2010). In particular, the inconsistencies include that 1) in BP, the feedback path is the reversal of the feedforward path in a way that the same synaptic weight parameters are used (a.k.a. weight transport problem (Grossberg 1987)), while the brain most likely uses different sets of parameters in the feedforward and feedback processes; 2) in BP, the layer-to-layer operations are asymmetric between feedforward and feedback processes (*i.e.*, the feedback process does not require the activation used in the feedforward process), while the brain

requires symmetric operations. Although there are on-going research efforts to connect the brain and BP (Lillicrap et al. 2020), many researchers seek less inconsistent yet practical algorithms of network training (Lillicrap et al. 2016; Bengio 2014; Lee et al. 2015; Bengio 2020; Meulemans et al. 2020; Ahmad, van Gerven, and Ambrogioni 2020; Scellier and Bengio 2017) because biologically plausible algorithms that may bridge the gap between neuroscience and computer science are believed to enhance machine learning.

Feedback alignment (FA) (Lillicrap et al. 2016) was proposed to resolve the weight transport problem by using fixed random weights for error propagation. It is worth noting that FA has been shown to outperform BP on real datasets, although the results are somewhat outdated (Nøkland 2016; Crafton et al. 2019).

Target propagation (TP) (Bengio 2014; LeCun 1986) has been proposed as a NN training algorithm that can circumvent the inconsistencies 1) and 2). The main idea of TP is to define target values for hidden neurons in each layer in a way that the *target values* (not the *error*) are backpropagated from the output layer down to the first hidden layer, using the same activation function used in the feedforward process. The feedback network, which does *not* share parameters with the feedforward network, is trained so that each layer becomes an approximated inverse of the corresponding layer of the feedforward network, whereas the parameters of the feedforward network are updated to achieve the layer-wise target. In TP, the feedback network ideally realizes layer-wise autoencoders with the feedforward network, but in reality it often ends up with imperfect autoencoders, which could cause optimization problems (Lee et al. 2015; Meulemans et al. 2020). Among the methods that alleviate such small discrepancies (Lee et al. 2015; Bengio 2020), difference target propagation (DTP) (Lee et al. 2015) introduces linear correction terms to the feedback process and significantly improved the recognition performance of TP.

However, while the formalism of DTP to compute layer-wise targets with a feedback network is theoretically sound, training the feedback network is often demanding in the following aspects: a) Synchronous training of the feedforward and feedback networks often requires careful hyperparameter tuning (Bartunov et al. 2018). b) Training of the feedback network could be computationally very expensive. According to previous work (Bartunov et al. 2018; Meulemans et al.

2020; Ernoult et al. 2022), weight updates of the feedback networks were more frequent than those of the feedforward networks. In the latest research (Ernoult et al. 2022), the number of updating feedback weights is set to several tens of times of that of the feedforward weights. For these reasons, training a feedback network typically requires a large cost including hyperparameter tuning.

It is clear that having a relation of layer-wise autoencoders by the feedforward and feedback network is sufficient for the target propagation algorithms to gain training capability. In this work, we aim to answer the question whether constructing layer-wise autoencoders is also a *necessary* condition for target propagation to work. To answer this question, we examined a very simple approach, where the parameters of the feedback network are kept fixed while the feedforward network is trained just as DTP. No reconstruction loss is imposed, so the feedforward and feedback networks are not forced to form autoencoders. Nevertheless, our new target propagation method, *fixed-weight difference target propagation* (FW-DTP), greatly improves the stability of training and test performance compared to DTP while reducing computational complexity from DTP. The idea of fixing feedback weights is inspired by FA, which fixes feedback weights during BP to avoid the weight transport problem. But the difference is that FW-DTP greatly simplifies the learning rule of DTP by removing layer-wise autoencoding losses, whereas FA has no such effect. We provide mathematical expressions about conditions that network trained with DTP will implicitly acquire with and without fixing feedback weights. We further propose a novel propagation architecture which can explicitly provide the exact form of the feedback function of DTP, which implies that FW-DTP acquires implicit autoencoders. It is worth mentioning that Local Representation Alignment (LRA) (Ororbia et al. 2018) (followed by (Ororbia and Mali 2019; Ororbia et al. 2020)) also proposed biologically-plausible layer-wise learning rules with fixed parameters, though it does not belong to the target propagation family.

Our contribution is three-fold: **1)** We propose *fixed-weight difference target propagation* (FW-DTP) that fixes feedback weights and drops the layer-wise autoencoding losses from DTP. Good learnability of FW-DTP indicates that optimizing the objectives of layer-wise target reconstruction is not necessary for the concept of target propagation to properly work. **2)** We present a novel architecture that explicitly shows the exact form of feedback function of DTP, which allows for an accurate notation of how the targets are back-propagated in the feedback network. **3)** We experimentally show that FW-DTP not only improves the stability of training from DTP, but also improves the mean test accuracies from DTP on four image classification datasets just like FA outperforming BP by using fixed backward weights.

2 Overview: Target Propagation Methods

We overview target propagation methods including TP (Bengio 2014) and DTP (Lee et al. 2015).

Definition 2.1 (Feedforward and feedback functions). Let \mathcal{X} and \mathcal{Y} be the input and output spaces, respectively. A

feedforward function $F : \mathcal{X} \rightarrow \mathcal{Y}$ is defined as a composite function of layered encoders f_l ($l = 1, \dots, L$) by

$$F(x) = f_L \circ f_{L-1} \circ \dots \circ f_1(x) \quad (1)$$

where L is the number of encoding layers, $x \in \mathcal{X}$ is an input. A feedback function $G : \mathcal{Y} \rightarrow \mathcal{X}$ is defined by

$$G(y) = g_1 \circ g_2 \circ \dots \circ g_L(y) \quad (2)$$

where $y \in \mathcal{Y}$ is an output and g_l is the l -th decoder. Each g_l is paired with f_l , and will be trained to approximately invert f_l . The feedforward activation h_l is recursively defined as

$$h_l = \begin{cases} x & (l = 0) \\ f_l(h_{l-1}) & (l = 1, \dots, L) \end{cases} \quad (3)$$

and the target τ_l is recursively defined in the descending order as

$$\tau_l = \begin{cases} y^* & (l = L) \\ \tilde{g}_{l+1}(\tau_{l+1}) & (l = L - 1, \dots, 0) \end{cases} \quad (4)$$

where y^* is the output target. In Eq. (4), \tilde{g}_l is an extended function of g_l to propagate targets, and it could be the same as g_l . Note that this paper focuses on supervised learning where loss $\mathcal{L}(F(x), y)$ to be minimized takes finite values over all training pairs $(x, y) \in \mathcal{X} \times \mathcal{Y}$.

Target Propagation (TP). TP is an algorithm to learn the feedforward and feedback function where f_l and g_l are parameterized. It defines the output target based on gradient descent (GD) (Bengio 2014) as

$$y^*(h_L) = h_L - \beta \frac{\partial \mathcal{L}(h_L, y)}{\partial h_L} \quad (5)$$

where β is a nudging parameter. For propagating targets, $\tilde{g}_l = g_l$ is used. TP updates feedforward weights (the parameters of f_l) and feedback weights (the parameters of g_l) alternately. The l -th layer's feedforward weight is updated to reduce layer-wise local loss:

$$L_l = \frac{1}{2\beta} \|h_l - \tau_l\|_2^2 \quad (6)$$

where τ_l is considered as a constant with respect to the l -th layer's feedforward weight, *i.e.*, the gradient of τ_l with respect to the weight is 0. The l -th layer's feedback weight is updated to reduce reconstruction loss:

$$L'_l = \frac{1}{2} \mathbb{E}_{\epsilon \sim \mathcal{N}(0, \sigma^2 I)} [\|h_{l-1} + \epsilon - g_l \circ f_l(h_{l-1} + \epsilon)\|_2^2] \quad (7)$$

where ϵ is a small noise to improve the robustness of inversion. A known limitation of TP is that imperfectness of the feedback function as inverse leads to a critical optimization problem (Lee et al. 2015; Meulemans et al. 2020), *i.e.*, the update direction $\tau_l - h_l$ involves reconstruction errors $g_{l+1}(f_{l+1}(h_l)) - h_l$; thus, the feedforward network is not trained properly with an imprecisely optimized feedback network.

Difference Target Propagation (DTP). Lee *et al.* (Lee et al. 2015) show that *difference correction*, subtracting the difference $g_{l+1}(h_{l+1}) - h_l$ from the target, alleviates the limitation of TP, and they introduce DTP, whose function \tilde{g}_{l+1} for propagating targets in Eq. (4) is defined by

$$\tilde{g}_{l+1}(\tau_{l+1}) = g_{l+1}(\tau_{l+1}) + h_l - g_{l+1}(h_{l+1}). \quad (8)$$

The losses for updating feedforward and feedback weights are the same as those of TP. In DTP, assuming all encoders are invertible, the first order approximation of $\Delta h_l := \tau_l - h_l$ is given by

$$\Delta h_l \simeq \left[\prod_{k=l+1}^L \frac{\partial g_k(h_k)}{\partial h_k} \right] \Delta h_L \quad (9)$$

$$= \left[\prod_{k=l+1}^L J_{g_k} \right] \left(-\beta \frac{\partial \mathcal{L}(h_L, y)}{\partial h_L} \right) \quad (10)$$

$$= -\beta J_{f_{l+1:L}}^{-1} \frac{\partial \mathcal{L}(h_L, y)}{\partial h_L} \quad (11)$$

where $J_{g_k} := \partial g_k(h_k) / \partial h_k$ is the Jacobian matrix of g_k evaluated at h_k . Here, $J_{g_l} = J_{f_l}^{-1}$ ($l = 1, \dots, L$) and $J_{f_{l+1:L}}^{-1} = \prod_{k=l+1}^L J_{f_k}^{-1}$ are used due to the invertibility, where $J_{f_l} := \partial f_k(h_{k-1}) / \partial h_{k-1}$ is the Jacobian matrix of f_k evaluated at h_{k-1} . The notation $()_{a:b}$ is for composing functions from layers a to b , e.g., $f_{l+1:L} = f_L \circ \dots \circ f_{l+1}$. The update rule of DTP is regarded as a hybrid of GD and Gauss-Newton (GN) algorithm (Gauss 1809). Note that, in the case of the *non-invertible* encoders, DTP obtains the condition $J_{g_l} = J_{f_l}^+$ where $J_{f_l}^+$ is the Moore-Penrose inverse (Moore 1920; Penrose 1955) of J_{f_l} , however, $J_{f_{l+1:L}}^+ = \prod_{k=l+1}^L J_{f_k}^+$ is not always satisfied (Meulemans et al. 2020; Campbell and Meyer 2009).

3 Proposed Method

This section presents the proposed fixed-weight difference target propagation (FW-DTP) that drops the training of feedback weights. We first propose FW-DTP according to the traditional notation (defined in Section 2) in 3.1. We then analyze FW-DTP from two points of view: the conditions for Jacobians in 3.2 and the exact form of the feedback function in 3.3. From these analyses, we explain why fixed-weights of FW-DTP has a good learnability.

3.1 Fixed-Weight Difference Target Propagation

FW-DTP is defined as the algorithm that omits reconstruction loss for updating feedback weights in DTP. All feedback weights are first randomly initialized and then fixed during training. For example, with a fully connected network, the l -th encoder and decoder of FW-DTP are defined by

$$f_l(h_{l-1}) := \sigma_l(W_l h_{l-1}), \quad g_l(\tau) := \sigma'_l(B_l \tau) \quad (12)$$

where σ and σ' are non-linear activation functions and W_l and B_l are matrices which denote the feedforward and feedback weights, respectively. B_l is first initialized with a distribution $P(B_l)$ and then fixed, while W_l is updated in

the learning process. The feedback propagation of targets are defined by Eq. (8). Note that DTP asymptotically approaches FW-DTP by decreasing the learning rate of the feedback weights. This is discussed with experimental results in the appendix.

3.2 Analysis 1: Condition for Jacobians

Here, we discuss conditions for DTP to appropriately work. Given that precise inverse relation between f_l and g_l may not be always obtainable in DTP, training with inaccurate targets can degrade the overall performance of the feedforward function. Now, consider two directions $\tau_l - h_l$ and $f_l(h_{l-1}^*) - h_l$, a vector from the activation h_l to the target τ_l at layer l , and another from h_l to the point $f_l(h_{l-1}^*)$. If the condition

$$-\frac{\pi}{2} \leq \angle(\tau_l - h_l, f_l(h_{l-1}^*) - h_l) \leq \frac{\pi}{2} \quad \text{where } h_{l-1}^* = \tau_{l-1} \quad (13)$$

holds, *i.e.*, if the angle between them is within 90 degrees, the loss of this sample is expected to decrease because $f_l(h_{l-1}^*)$ is the best point achieved by learning $(l-1)$ -th encoder. By applying the first order approximation, Eq. (13) is rewritten as

$$\Delta h_l^\top J_{f_l} J_{g_l} \Delta h_l \geq 0 \quad (14)$$

therefore, the sufficient condition of Eq. (13) is that $J_{f_l} J_{g_l}$ is a positive semi-definite matrix. As Table 1 shows, minimization of reconstruction losses of DTP such as original DTP (Eq. (7)), difference reconstruction loss (DRL) (Meulemans et al. 2020) and local difference reconstruction loss (L-DRL) (Ernoult et al. 2022) naturally satisfy the positive semi-definiteness by enforcing the Jacobian matrix J_{g_l} as the inverse or transpose of J_{f_l} . On the other hand, positive semi-definiteness requires

$$\inf_{\epsilon} [\epsilon^\top J_{f_l} J_{g_l} \epsilon] \geq 0 \quad (15)$$

however, this condition could be somewhat too strict, given that features may not always span the full space. In FW-DTP, the strict condition expressed in Eq. (15) is not generally satisfied because FW-DTP has no feedback objective function to learn to explicitly satisfy this condition. Now, let us consider a hypothetical situation where the product of Jacobians satisfies the condition,

$$\mathbb{E}_{\epsilon \sim p(\cdot)} [\epsilon^\top J_{f_l} J_{g_l} \epsilon] \geq 0 \quad (16)$$

where the infimum in Eq. (15) is replaced with the expectation over some origin-centric rotationally-symmetric distribution $p(\cdot)$ such as a zero-mean isotropic Gaussian distribution. Then, it is straightforward to show that Eq. (16) is equivalent to

$$\text{tr}(J_{f_l} J_{g_l}) \geq 0 \quad (17)$$

(the proof is in Appendix B). The condition expressed in Eq. (17) is weaker than Eq. (15). Under the condition of Eq. (17), if $(l-1)$ -th activation moves toward the target, it will shift l -th activation toward the corresponding target within $\pi/2$ range as the expectation (over p). Although the

condition of Eq. (17) is somewhat artificial, but indeed we found that FW-DTP does satisfy this condition in our experiment as we show in Section 4. The condition expressed in Eq. (17) could be regarded as a type of alignments that the network implicitly acquires when its feedback weights are fixed during DTP updates.

3.3 Analysis 2: Exact Form of Feedback Function

To show how targets are propagated in FW-DTP, we present a propagation architecture which provides the exact form of the feedback function of DTP. There exists no autoencoders in FW-DTP at least explicitly; however, difference correction creates autoencoders implicitly. To explicitly show this, instead of using the function \tilde{g}_l for propagating targets in Eq (4), we decomposed encoder and decoder as $f_l = f_l^\nu \circ f_l^\mu$ and $g_l = g_l^\nu \circ g_l^\mu$ to incorporate the difference correction mechanism into g_l^ν . Using the proposed architecture represented by Eqs. (18-20), TP and DTP are reformulated as Eqs. (22-30) and the training process is also reformulated as Eq. (21).

Definition 3.1 (Propagation Architecture). We define a feedforward function $F : \mathcal{X} \rightarrow \mathcal{Y}$ with encoders f_l and a feedback function $G : \mathcal{Y} \rightarrow \mathcal{X}$ with decoders g_l by Eqs. (1-2). The targets are recursively defined in the descending order as

$$\tau_l = \begin{cases} y^* & (l = L) \\ g_{l+1}(\tau_{l+1}) & (l = L - 1, \dots, 0) \end{cases} \quad (18)$$

where y^* is the output target. Eq (18) differs from Eq (4) in that we avoid to define \tilde{g}_l . Further, we introduce four functions $f_l^\mu, f_l^\nu, g_l^\mu, g_l^\nu$ that decompose the encoder and decoder into

$$f_l = f_l^\nu \circ f_l^\mu, \quad g_l = g_l^\nu \circ g_l^\mu. \quad (19)$$

We also define a shortcut function ψ_l that map the activation to the target as

$$\psi_l(h_l) = \begin{cases} \tau_L & (l = L) \\ g_{L:l+1} \circ \psi_L \circ f_{l+1:L}(h_l) & (l = L - 1, \dots, 0). \end{cases} \quad (20)$$

Here, $\psi_l(h_l) = \tau_l$. Figure 1a illustrates the proposed propagation architecture. With this architecture, we expect that $g_l \circ f_l$ will become an autoencoder after convergence with the activations sufficiently close to the corresponding targets. It is reduced to DTP when f_l^μ is the identity function, f_l^ν is a parameterized function (e.g., $f_l^\nu(h_{l-1}) = \sigma(W_l h_{l-1})$), g_l^μ is another parameterized function, and g_l^ν is a function of difference correction, as shown in Figure 1b and 1c. Note that Figure 1c is a well-known visualization of DTP (Lee et al. 2015). The main problem we would like to discuss is whether there exists the exact form of g_l^ν . With the traditional notations in Eq. (8), \tilde{g}_{l+1} is defined as a function of τ_{l+1} , however, it uses h_l and h_{l+1} in the right side of the equation. This makes it difficult to analyze the shape of feedback function; thus, we define the training process here as follows.

Definition 3.3 (Training). Let $q_l = (f_l^\mu, f_l^\nu, g_l^\mu, g_l^\nu)$ a quadruplet of functions. We define training as the process

to solve the following layer-wise problem:

$$q_l^* = \operatorname{argmin}_{q_l \in \Omega_l} \mathcal{O}_l \quad (21)$$

where $\Omega_l = \mathcal{F}_l^\mu \times \mathcal{F}_l^\nu \times \mathcal{G}_l^\mu \times \mathcal{G}_l^\nu$ is a function space (search space), and \mathcal{O}_l is the objective function.

This definition involves TP and DTP variants as follows.

Target Propagation. Using the proposed architecture, TP is defined as a training process with the search spaces:

$$\mathcal{F}_l^\mu = \{id\}, \quad \mathcal{F}_l^\nu = \{p_\theta : \theta \in \Theta_l\} \quad (22)$$

$$\mathcal{G}_l^\mu = \{p_\omega : \omega \in \Omega_l\}, \quad \mathcal{G}_l^\nu = \{id\} \quad (23)$$

where id is the identity function and p_θ and p_ω are parameterized functions with learnable parameters θ and ω , respectively. Θ_l and Ω_l are the parameter spaces. TP solves Eq. (21) by alternately solving two problems:

$$f_l^{\nu*} = \operatorname{argmin}_{f_l^\nu \in \mathcal{F}_l^\nu} \mathcal{O}_l^{(1)} \quad (24)$$

$$g_l^{\mu*} = \operatorname{argmin}_{g_l^\mu \in \mathcal{G}_l^\mu} \mathcal{O}_l^{(2)} \quad (25)$$

where $\mathcal{O}_l^{(1)}$ is the layer-wise local loss in Eq. (6) and $\mathcal{O}_l^{(2)}$ is the reconstruction loss in Eq. (7).

Difference Target Propagation. DTP is also defined with a search space \mathfrak{G}_l for g_l^ν as follows:

$$\mathcal{F}_l^\mu = \{id\}, \quad \mathcal{F}_l^\nu = \{p_\theta : \theta \in \Theta_l\} \quad (26)$$

$$\mathcal{G}_l^\mu = \{p_\omega : \omega \in \Omega_l\}, \quad \mathcal{G}_l^\nu = \mathfrak{G}_l \quad (27)$$

$$\text{where } \mathfrak{G}_l = \{g_l^\nu : d_P(f_l^\mu \circ g_l \circ \psi_l \circ f_l, g_l^\mu \circ \psi_l \circ f_l + f_l^\mu - g_l^\mu \circ f_l) = 0\} \quad (28)$$

and d_P with norm P (e.g., L_2 norm) is a distance in the function space.

Figure 1d shows the two functions $f_l^\mu \circ g_l \circ \psi_l \circ f_l$ and $g_l^\mu \circ \psi_l \circ f_l + f_l^\mu - g_l^\mu \circ f_l$ in blue and red, respectively; namely, \mathfrak{G}_l is the function subspace of g_l^ν where these two functions (the blue and red arrows in 1d) are equal. By assuming functions f_l^ν, ψ_l, g_l^μ are bijective, we have $\mathfrak{G}_l = \{\check{g}_l^\nu\}$ where

$$\check{g}_l^\nu = id + (f_l^\nu)^{-1} \circ (\psi_l)^{-1} \circ (g_l^\mu)^{-1} - g_l^\mu \circ (\psi_l)^{-1} \circ (g_l^\mu)^{-1}. \quad (29)$$

This is the exact form of difference correction in our formulation. This shows that g_l^ν is implicitly updated by updating f_l^ν and g_l^μ . Therefore, DTP solves Eq. (21) by alternately solving two problems:

$$(f_l^{\nu*}, g_l^{\nu*}) = \operatorname{argmin}_{(f_l^\nu, g_l^\nu) \in \mathcal{F}_l^\nu \times \mathcal{G}_l^\nu} \mathcal{O}_l^{(1)}, \quad (g_l^{\mu*}, g_l^{\nu*}) = \operatorname{argmin}_{(g_l^\mu, g_l^\nu) \in \mathcal{G}_l^\mu \times \mathcal{G}_l^\nu} \mathcal{O}_l^{(2)} \quad (30)$$

where the objective function is the same as that of TP. Eq. (30) indicates that updating the feedforward weights implicitly update g_l^ν in the feedback path.

Fixed-Weight Difference Target Propagation. From Eq. (29), we notice that *DTP works even with fixed g_l^μ* because g_l^ν is updated in conjunction with f_l^ν . If the function

Table 1: The conditions of the Jacobians obtained by various reconstruction losses and FW-DTP.

METHOD	DTP	DRL	L-DRL	FW-DTP
CONDITION	$J_{g_l} = J_{f_l}^+$	$\prod_{k=l}^L J_{g_k} = J_{f_{l:L}}^+$	$J_{g_l} = J_{f_l}^\top$	$\text{tr}(J_{f_l} J_{g_l}) > 0$

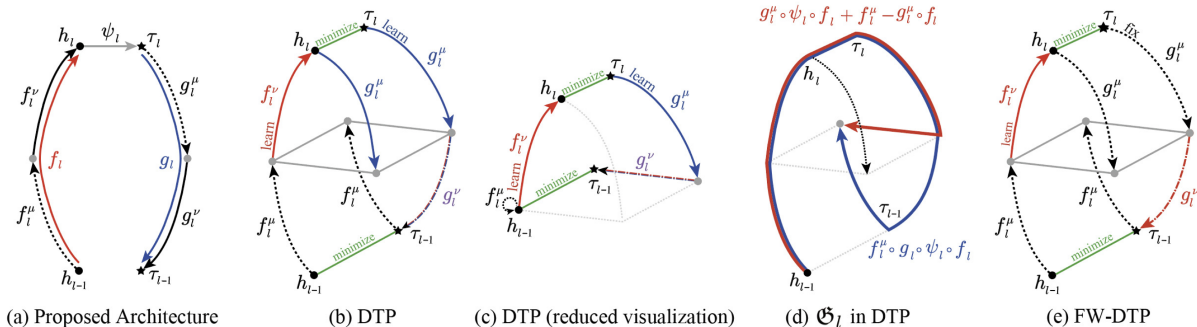


Figure 1: Proposed propagation architecture and its reduction to DTP. (a) The proposed architecture. The encoder f_l is decomposed into f_l^μ and f_l^ν . The decoder g_l is decomposed into g_l^μ and g_l^ν . ψ_l is the shortcut function from an activation h_l to the target τ_l . (b) Reduction to DTP. g_l^ν is a function of difference correction. f_l^μ is illustrated as non-identity function. (c) Reduction to DTP, where f_l^μ is illustrated as the identity function. This is the well-known visualization of DTP. (d) The search space \mathcal{G}_l in DTP. (e) FW-DTP with fixed g_l^μ

space \mathcal{F}_l^ν is large enough for finding an appropriate pair of f_l^ν and g_l^ν , parametrization of the two function spaces \mathcal{F}_l^ν and \mathcal{G}_l^μ may be redundant. Based on this observation, FW-DTP uses a unit set for \mathcal{G}_l^μ :

$$\mathcal{F}_l^\mu = \{id\}, \mathcal{F}_l^\nu = \{p_\theta : \theta \in \Theta_l\}, \mathcal{G}_l^\mu = \{r_l\}, \mathcal{G}_l^\nu = \mathcal{G}_l \quad (31)$$

where r_l is a fixed random function. FW-DTP solves Eq. (21) by solving one problem:

$$(f_l^{\nu*}, g_l^{\nu*}) = \underset{(f_l^\nu, g_l^\nu) \in \mathcal{F}_l^\nu \times \mathcal{G}_l^\nu}{\text{argmin}} \mathcal{O}_l^{(1)}. \quad (32)$$

Figure 1e shows that in FW-DTP, g_l^μ is fixed but g_l^ν colored in red moves with f_l^ν , and thus there still exists an auto-encoder $g_l \circ f_l$. This is one of the reasons why FW-DTP has an ability to propagate targets to decrease loss. To keep non-linearity and the ability to entangle elements from different dimension on the feedback path, $r_l(a) = \sigma(B_l a)$ would be the simplest choice where B_l is a random matrix fixed before training and σ is a non-linear activation function. FW-DTP is more efficient than DTP because it reduces the number of learnable parameters.

4 Experiments

In this section, we show experimental results.¹ First, we show that the weak condition expressed in Eq. (16) is satisfied by FW-DTP experimentally. We then compare FW-DTP with TP and DTP variants. Lastly, we evaluate the hyperparameter sensitivity and computational cost, and show that

¹Our code is available at <https://github.com/TatsukichiShibuya/Fixed-Weight-Difference-Target-Propagation>.

FW-DTP is more stable and computationally efficient than DTP.

4.1 Weak and Strict Conditions of Jacobians

Experimental set-up. This experiment aims to show that FW-DTP satisfies the weak condition of Jacobians given by Eq. (16) during its training process. We also show that FW-DTP does not satisfy the strict condition expressed in Eq. (15) in contrast to DTP.

Evaluation details are as follows. For the weak condition, we directly measured the trace of $J_{f_l} J_{g_l}$ (With notations in Analysis 2, this is $J_{f_l^\nu} J_{g_l^\mu}$). For the strict condition, we measured the proportion of the number of non-negative eigenvalues of $J_{f_l} J_{g_l}$ to its dimension. This is a measure of positive semi-definiteness. The MNIST dataset (Lecun et al. 1998) was used for this evaluation. A fully connected network with 6 layers each with 256 units was trained with cross-entropy loss. Note that the first and the last encoders are non-invertible due to the difference of the input and output dimensions. We chose the hyperbolic tangent as the activation function, but only for FW-DTP, batch normalization (BN) (Ioffe and Szegedy 2015) was applied after each hyperbolic tangent. The necessity and effectiveness of BN is discussed in the appendix. Stochastic gradient descent (SGD) was used as the optimizer. Details of the hyperparameters are also provided in the appendix. The feed-forward and feedback weights were initialized with random orthogonal matrices and random numbers from uniform distribution $U(-0.01, 0.01)$, respectively.

Results. Figure 2 shows the results of the last (sixth) layer and the second layer as representatives of intermediate layers. In Figure 2a, we see that the trace of $J_{f_l} J_{g_l}$ is positive

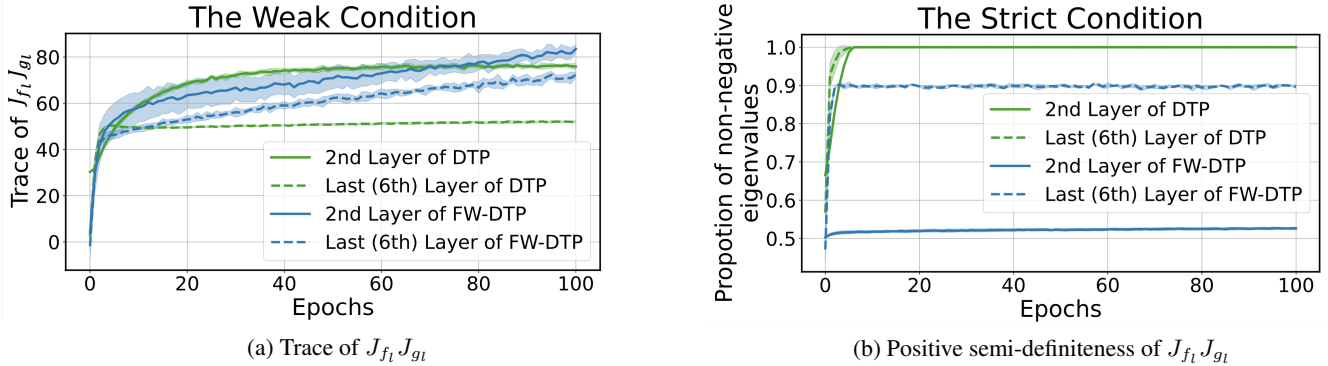


Figure 2: The Jacobian conditions of FW-DTP and DTP on MNIST with the mean and standard deviation over five different seeds. (a) Trace of $J_{f_i} J_{g_l}$ (the values of the trace on the 2nd layer of DTP are scaled by 0.1). We see that all values are positive. (b) The proportion of non-negative eigenvalues. We see the difference between DTP and FW-DTP.

from the first epoch, and is increasing during training process of DTP and FW-DTP. In contrast, in Figure 2b, we see the difference between DTP and FW-DTP. With DTP, all eigenvalues are non-negative after the tenth epoch on both layers. On the other hand, with FW-DTP, some of eigenvalues are negative. We see that $\approx 90\%$ of eigenvalues are non-negative in the last layer, but only $\approx 53\%$ of them are non-negative in the second layer.

These results confirm that FW-DTP satisfies only the weak condition expressed in Eq. (16) automatically, while DTP satisfies both of the weak and strict conditions.

4.2 Comparison with TP and DTP Variants

Experimental set-up. The purpose of this experiment is to demonstrate that the performance of FW-DTP is comparable with or even better than that of DTP. We compared image classification performance of TP (Bengio 2014), DTP (Lee et al. 2015), DRL (Meulemans et al. 2020), L-DRL (Ernoul et al. 2022), and FW-DTP on four datasets: MNIST (Lecun et al. 1998), Fashion-MNIST (F-MNIST) (Xiao, Rasul, and Vollgraf 2017), CIFAR-10 and CIFAR-100 (Krizhevsky 2009). Following previous studies (Bartunov et al. 2018; Meulemans et al. 2020), a fully connected network consists of 6 layers each with 256 units was used for MNIST and F-MNIST. Another fully connected network consists of 4 layers each with 1,024 units was used for CIFAR-10/100. Because FW-DTP halves the number of the learnable parameters by fixing the feedback weights, we also report results with a half number of learnable parameters with DTP, DRL and L-DRL. The activation function and the optimizer were the same as those used in 4.1. Details of the hyperparameters are provided in the appendix.

Results. The results are summarized in Table 2. As can be seen, FW-DTP is comparable with DTP and its variants. FW-DTP outperformed DTP in all datasets. This supports that FW-DTP works as a training algorithm even if it does not satisfy the strict condition of Jacobians. This also confirms that even with fixed feedback weights, FW-DTP propagates targets to decrease cross-entropy loss via the feedback path with the function g'_l for difference correction. Compar-

ison with DRL and L-DRL showed some limitation of FW-DTP. FW-DTP outperformed them on MNIST, F-MNIST, and CIFAR-10 when the number of learnable parameters was the same. On CIFAR-100, the test error of FW-DTP was not the best among them. However, when the number of parameters was the same, the difference in the test error between DTP and DRL or L-DRL was only $\leq 0.1\%$. Note that the goal of this study is not to outperform them but to analyze how and why FW-DTP works as a training algorithm with empirical evidence.

4.3 Hyperparameter Sensitivity and Computational Efficiency

Here, we investigate hyperparameter sensitivity and the computational cost of FW-DTP.

Hyperparameter sensitivity. We investigate how sensitive DTP and FW-DTP are to different hyperparameters. Namely, we tested 100 different random configurations. More specifically, denoting by $\alpha \in \mathbb{R}^H$ the flattened hyperparameters where H is the number of hyperparameters, each α_i was randomly sampled so that $\log(\alpha_i) \sim U(\log(0.2\bar{\alpha}_i), \log(5\bar{\alpha}_i))$ where U is the uniform distribution and $\bar{\alpha}$ is the hyperparameter used in 4.2. (see Appendix G for details). The histograms of the test accuracies on CIFAR-10 are visualized in Figure 3. As can be seen, FW-DTP is less sensitive than DTP to hyperparameters. This is because DTP needs the complicated interactions between feedforward and feedback training, as discussed in the previous work (Bartunov et al. 2018), while FW-DTP drops these complexities by relaxing the conditions of Jacobians from the strict one to the weak one.

Computational Cost. We compare the computational cost of each method on CIFAR-10 in Table 3. 4 GPUs (Tesla P100-SXM2-16GB) with 56 CPU cores are used to measure computational time. For DTP, DRL and L-DRL, the feedback weights are updated five times in each iteration. FW-DTP is ≈ 3.0 times slower than BP and > 3.7 times faster than DTP. This shows that BP is still better in terms of computational cost, however, FW-DTP is one of the most efficient methods in DTP variants. More detailed settings are

Table 2: Test error (%) obtained on four image classification datasets reported with the mean and standard deviation over five different seeds. For the hyperparameter search, 5,000 samples from the training set are used as the validation set. The best and the second best results are marked in bold and with an underline, respectively. The columns of #PARAMS is the number of learnable parameters (the sum of numbers of feedforward and the feedback networks).

METHODS	#PARAMS	MNIST	F-MNIST	#PARAMS	CIFAR-10	CIFAR-100
BP	0.5M	1.85±0.09	10.42±0.08	6.3M	46.16±1.15	75.96±0.52
FA (LILLICRAP ET AL. 2016)	0.5M	2.94±0.09	12.58±0.35	6.3M	51.33±0.81	77.43±0.21
TP	1.1M	78.99±2.04	—	13.0M	—	—
DTP (LEE ET AL. 2015)	0.5M	3.24±0.15	11.86±0.14	6.3M	52.17±0.79	77.89±0.39
	1.1M	<u>2.77±0.10</u>	<u>11.77±0.16</u>	13.0M	52.01±0.80	77.11±0.20
DRL (MEULEMANS ET AL. 2020)	0.5M	3.13±0.03	12.75±0.52	6.3M	50.11±0.67	76.69±0.30
	1.1M	2.84±0.09	12.15±0.25	13.0M	48.79±0.58	<u>75.62±0.35</u>
L-DRL (ERNOULT ET AL. 2022)	0.5M	3.14±0.03	12.45±0.36	6.3M	49.58±0.33	76.72±0.26
	1.1M	2.82±0.10	12.29±0.46	13.0M	49.84±0.55	75.62±0.31
FW-DTP	0.5M	2.76±0.10	11.76±0.37	6.3M	<u>48.97±0.32</u>	76.76±0.45

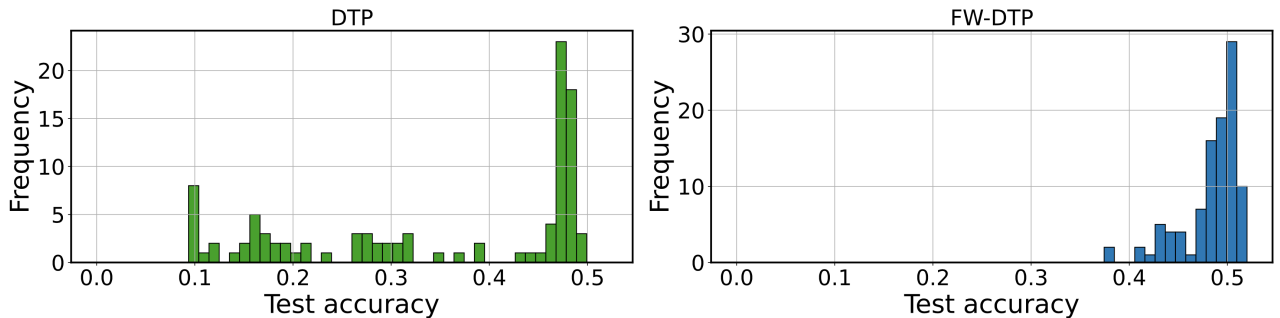


Figure 3: Histogram of test accuracies achieved under different hyperparameters on CIFAR-10.

Table 3: Training time [sec] per epoch of FW-DTP, DTP, DRL, L-DRL and BP on CIFAR-10.

	TIME[SEC]	RATIO TO FW-DTP	ERROR[%]
FW-DTP	2.22±0.02	1.00±0.00	48.97±0.32
DTP	8.32±0.36	3.74±0.17	52.01±0.80
DRL	9.52±0.08	4.29±0.05	48.79±0.58
L-DRL	8.86±0.08	3.99±0.05	49.84±0.55
BP	0.76±0.03	0.34±0.01	46.16±1.15

described in the appendix.

5 Discussion

In this paper, we proposed FW-DTP, which fixes feedback weights during training, and experimentally confirmed that its test performance is consistently better than that of DTP on four image-classification datasets, while the hyperparameter sensitivity and the computational cost are reduced. Further, we showed the strict and weak conditions of Jacobians, by which we explained the difference between FW-DTP and DTP. Finally, we discuss limitations and future work.

Biological plausibility. A limitation of FW-DTP is that it does not fulfill some biological constraints such as Dale’s

law (Parisien, Anderson, and Eliasmith 2008) and spiking networks (Samadi, Lillicrap, and Tweed 2017; Guerguiev, Lillicrap, and Richards 2017; Bengio et al. 2008). We have shown in Analysis 2 that the composite function $f_l \circ g_l$ forms a layer-wise autoencoder even with fixed feedback weights because we have a function g_l^v derived from difference correction. However, allowing $g_l^v \neq id$ may harm biological plausibility. Notably, this is not a problem only for FW-DTP. If we apply DTP to a non-injective feedforward function, a non-identity function g_l^v often remains. We hope our exact formulation of DTP helps researchers to analyze the behaviour of DTP in future.

Scalability. Another limitation in this work is that all of the four datasets are for image classification and are relatively small. We chose them because of two reasons: 1) they are suitable for analyzing Jacobian matrices during training to see the difference between FW-DTP and DTP, and 2) they are suitable for repeating many experiments with different hyper-parameters for evaluating the sensitivity. Recently, some improved targets propagated beyond layers (Meulemans et al. 2020; Ernoult et al. 2022) perform comparable with BP on large-scale datasets. From the point of view of fixed feedback weights, these methods may be related to the direct feedback alignment (Nøkland 2016; Crafton et al. 2019). Exploring a method to add such feedback paths efficiently with some fixed feedback weights would be an inter-

esting and necessary direction for future work.

New research direction. In this study, we assumed $f_l^\mu = id$ in the decomposed encoder for a fair comparison of FW-DTP with DTP and its variants. However, it is worth noting that exploring non-identity fixed function f_l^μ , as well as exploring different restrictions to the function space \mathfrak{D}_l would open a new research direction. In particular, the following symmetry in FW-DTP would be effective to explore new biologically plausible function families: f_l^μ, g_l^μ are fixed, and f_l^ν, g_l^ν are determined by a parameter θ . This direction includes research topics about how to fix weights in conjunction with feedback alignment methods (Crafton et al. 2019; Moskovitz, Litwin-Kumar, and Abbott 2018; Garg and Vempala 2022), and how to parameterize paired functions with some reparametrization tricks. Under the weak condition of Jacobians, there must be fruitful function families that have never been investigated for propagating targets.

Acknowledgement

This work was an outcome of a research project, Development of Quality Foundation for Machine-Learning Applications, supported by DENSO IT LAB Recognition and Learning Algorithm Collaborative Research Chair (Tokyo Tech.). This work was also supported by JSPS KAKENHI Grant Number JP22H03642.

References

- Ahmad, N.; van Gerven, M.; and Ambrogioni, L. 2020. GAIT-prop: A biologically plausible learning rule derived from backpropagation of error. In *NeurIPS*.
- Bartunov, S.; Santoro, A.; Richards, B.; Marris, L.; Hinton, G.; and Lillicrap, T. 2018. Assessing the Scalability of Biologically-Motivated Deep Learning Algorithms and Architectures. In *NeurIPS*.
- Bengio, Y. 2014. How auto-encoders could provide credit assignment in deep networks via target propagation. *arXiv preprint arXiv:1407.7906*.
- Bengio, Y. 2020. Deriving Differential Target Propagation from Iterating Approximate Inverses. *arXiv preprint arXiv:2007.15139*.
- Bengio, Y.; Mesnard, T.; Fischer, A.; Zhang, S.; and Wu, Y. 2008. STDP-Compatible Approximation of Backpropagation in an Energy-Based Model. *Neural computation*.
- Campbell, S. L.; and Meyer, C. D. 2009. *Generalized inverses of linear transformations*. SIAM.
- Crafton, B.; Parihar, A.; Gebhardt, E.; and Raychowdhury, A. 2019. Direct feedback alignment with sparse connections for local learning. *Frontiers in Neuroscience*, 13.
- Crick, F. 1989. The recent excitement about neural networks. *Nature*, 337: 129–132.
- Ernault, M.; Normandin, F.; Moudgil, A.; Spinney, S.; Belilovsky, E.; Rish, I.; Richards, B.; and Bengio, Y. 2022. Towards Scaling Difference Target Propagation by Learning Backprop Targets. In *ICML*.
- Frenkel, C.; Lefebvre, M.; and Bol, D. 2021. Learning Without Feedback: Fixed Random Learning Signals Allow for Feedforward Training of Deep Neural Networks. *Frontiers in Neuroscience*, 10.
- Garg, S.; and Vempala, S. S. 2022. How and When Random Feedback Works: A Case Study of Low-Rank Matrix Factorization. *arXiv preprint arXiv:2111.08706*.
- Gauss, C. F. 1809. *Theoria motus corporum coelestium in sectionibus conicis solem ambientium*, volume 7. Perthes et Besser.
- Glorot, X.; and Bengio, Y. 2010. Understanding the difficulty of training deep feedforward neural networks. In *AIS-TATS*.
- Grossberg, S. 1987. Competitive learning: From interactive activation to adaptive resonance. *Cognitive Science*, 11: 23–63.
- Guerguiev, J.; Lillicrap, T. P.; and Richards, B. A. 2017. Towards deep learning with segregated dendrites. *ELife*, 6.
- Ioffe, S.; and Szegedy, C. 2015. Batch Normalization: Accelerating Deep Network Training by Reducing Internal Covariate Shift. In *ICML*.
- Krizhevsky, A. 2009. Learning multiple layers of features from tiny images. *Technical Report*.
- LeCun, Y. 1986. Learning processes in an asymmetric threshold network. *Disordered systems and biological organization*.
- Lecun, Y.; Bottou, L.; Bengio, Y.; and Haffner, P. 1998. Gradient-based learning applied to document recognition. *IEEE*, 86: 2278–2324.
- Lee, D.-H.; Zhang, S.; Fischer, A.; and Bengio, Y. 2015. Difference Target Propagation. In *ECML/PKDD*.
- Lillicrap, T.; Cownden, D.; Tweed, D.; and Akerman, C. 2016. Random synaptic feedback weights support error backpropagation for deep learning. *Nature Communications*, 7.
- Lillicrap, T.; Santoro, A.; Marris, L.; Akerman, C.; and Hinton, G. 2020. Backpropagation and the brain. *Nature*, 21: 335–346.
- McCulloch, W. S.; and Pitts, W. 1943. A logical calculus of the ideas immanent in nervous activity. *Bulletin of mathematical biophysics*, 5: 115–133.
- Meulemans, A.; Carzaniga, F. S.; Suykens, J. A.; Sacramento, J.; and Grewe, B. F. 2020. A theoretical framework for target propagation. In *NeurIPS*.
- Moore, E. H. 1920. On the reciprocal of the general algebraic matrix. *Bulletin of American Mathematical Society*, 26: 394–395.
- Moskovitz, T. H.; Litwin-Kumar, A.; and Abbott, L. 2018. Feedback alignment in deep convolutional networks. *arXiv preprint arXiv:1812.06488*.
- Nøkland, A. 2016. Direct Feedback Alignment Provides Learning in Deep Neural Networks. In *NeurIPS*.
- Ororbia, A. G.; and Mali, A. 2019. Biologically Motivated Algorithms for Propagating Local Target Representations. In *AAAI*.

- Ororbia, A. G.; Mali, A.; Giles, C. L.; and Kifer, D. 2020. Continual Learning of Recurrent Neural Networks by Locally Aligning Distributed Representations. *IEEE Transactions on Neural Networks and Learning Systems*.
- Ororbia, A. G.; Mali, A.; Kifer, D.; and Giles, C. L. 2018. Conducting Credit Assignment by Aligning Local Representations. *arXiv preprint arXiv:1803.01834*.
- Parisien, C.; Anderson, C. H.; and Eliasmith, C. 2008. Solving the problem of negative synaptic weights in cortical models. *Neural computation*, 20: 1473–1494.
- Penrose, R. 1955. A generalized inverse for matrices. *Mathematical proceedings of the Cambridge philosophical society*, 51: 406–413.
- Rosenblatt, F. 1958. The Perceptron: A Probabilistic Model for Information Storage and Organization in the Brain. *Psychological Review*, 65(6): 386–408.
- Rumelhart, D. E.; Hinton, G. E.; and Williams, R. J. 1986. Learning representations by back-propagating errors. *Nature*, 323: 533–536.
- Samadi, A.; Lillicrap, T. P.; and Tweed, D. B. 2017. Deep learning with dynamic spiking neurons and fixed feedback weights. *Neural computation*.
- Scellier, B.; and Bengio, Y. 2017. Equilibrium Propagation: Bridging the Gap between Energy-Based Models and Back-propagation. *Frontiers in computational neuroscience*, 11.
- Xiao, H.; Rasul, K.; and Vollgraf, R. 2017. Fashion-mnist: a novel image dataset for benchmarking machine learning algorithms. *arXiv preprint arXiv:1708.07747*.

A Formulation Details

This section presents the details of our formulations. We show that with DTP, non-injective feedforward functions lead to non-continuous feedback functions, and discuss pros and cons of updating feedback weights. We start from the definition of training.

Definition A.1 (Training). Let $f_l : \mathcal{X}_{l-1} \rightarrow \mathcal{X}_l$ and $g_l : \mathcal{X}_l \rightarrow \mathcal{X}_{l-1}$ be the l -th encoder and decoder, respectively, where \mathcal{X}_{l-1} is a non-empty set, and $\mathcal{X}_l = \text{Im} f_l$ (i.e., the codomain of f_l is defined so that f_l is surjective). Suppose they are decomposed into $f_l = f_l^\nu \circ f_l^\mu$ and $g_l = g_l^\nu \circ g_l^\mu$, where there exists two intermediate hidden spaces \mathcal{Z}_l and \mathcal{W}_l such that $f_l^\mu : \mathcal{X}_{l-1} \rightarrow \mathcal{Z}_l$, $f_l^\nu : \mathcal{Z}_l \rightarrow \mathcal{X}_l$, $g_l^\mu : \mathcal{X}_l \rightarrow \mathcal{W}_l$, and $g_l^\nu : \mathcal{W}_l \rightarrow \mathcal{X}_{l-1}$. Denoting by $\mathbf{q}_l = (f_l^\nu, f_l^\mu, g_l^\nu, g_l^\mu) \in \mathfrak{D}_l$ a quadruplet of the four functions, a *training step* is defined as the process to update it from $\mathbf{q}_l^{(t)}$ to $\mathbf{q}_l^{(t+1)}$ by solving or approximately solving the following problem:

$$\mathbf{q}_l^{(t+1)} = \underset{\mathbf{q}_l \in \mathfrak{D}_l^{(t)}[\mathbf{q}^{(t)}]}{\text{argmin}} \mathcal{O}_l^{(t)} \quad (33)$$

where $t \in \mathbb{N} = \{0, 1, 2, \dots\}$ is the time step, $\mathcal{O}_l^{(t)}$ is the objective function, and $\mathfrak{D}_l^{(t)}[\mathbf{q}^{(t)}] \subset \mathfrak{D}_l$ is the restricted function space (search space). Here, \mathfrak{D}_l is the whole search space given by a product space $\mathfrak{D}_l = \mathcal{F}_l^\nu \times \mathcal{F}_l^\mu \times \mathcal{G}_l^\nu \times \mathcal{G}_l^\mu$ where

$$\begin{aligned} \mathcal{F}_l^\nu &\subset \{f_l^\nu : \mathcal{Z}_l \rightarrow \mathcal{X}_l\}, \quad \mathcal{F}_l^\mu \subset \{f_l^\mu : \mathcal{X}_{l-1} \rightarrow \mathcal{Z}_l\}, \\ \mathcal{G}_l^\nu &\subset \{g_l^\nu : \mathcal{W}_l \rightarrow \mathcal{X}_{l-1}\}, \quad \mathcal{G}_l^\mu \subset \{g_l^\mu : \mathcal{X}_l \rightarrow \mathcal{W}_l\} \end{aligned} \quad (34)$$

are subsets of function spaces.

With this definition, the training step of target propagation (TP) is formulated as follows.

Definition A.2 (Target Propagation). Let p_θ and q_ω be two parameterized functions where $\theta \in \Theta$ and $\omega \in \Omega$ are parameters. Also, define parameterized function spaces p_Ω, p_Θ as $p_\Omega = \{p_\omega : \omega \in \Omega\}$, $p_\Theta = \{p_\theta : \theta \in \Theta\}$, respectively. The training step of TP is defined with the following search space \mathfrak{D}_l , the restricted search space $\mathfrak{D}_l^{(t)}$, and the objective function $\mathcal{O}_l^{(t)}$:

$$\begin{aligned} \mathfrak{D}_l &= \{(f_l^\nu, f_l^\mu, g_l^\nu, g_l^\mu) : \\ &\quad f_l^\nu \in p_\Theta, f_l^\mu = id, g_l^\nu = id, g_l^\mu \in p_\Omega\} \end{aligned} \quad (35)$$

where *id* is the identity function². Given an initial quadruplet $\mathbf{q}_l^{(0)} = (p_{\theta_0}, id, id, p_{\omega_0})$ with randomly chosen $\theta_0 \in \Theta$ and $\omega_0 \in \Omega$, the restricted search spaces for $t = 1, 2, \dots$ are defined as

$$\begin{aligned} \mathfrak{D}_l^{(t)}[\mathbf{q}^{(t)}] &= \left\{ \begin{aligned} &\{(f_l^\nu, id, id, g_l^\mu) : f_l^\nu \in p_\Theta, g_l^\mu = p_{\omega_t}\} \quad (t \in \mathbb{E}) \\ &\{(f_l^\nu, id, id, g_l^\mu) : f_l^\nu = p_{\theta_t}, g_l^\mu \in p_\Omega\} \quad (t \in \mathbb{O}) \end{aligned} \right. \end{aligned} \quad (36)$$

where \mathbb{E} is the set of even numbers, and \mathbb{O} is the set of odd numbers. This expresses that TP seeks new feedforward

²This assumes $\mathcal{Z}_l = \mathcal{W}_l = \mathcal{X}_{l-1}$.

weights θ_{t+1} and new feedback weights ω_{t+1} alternately. The objective function is also switched to alternately apply the layer-wise local loss and reconstruction loss as

$$\mathcal{O}_l^{(t)} = \begin{cases} \frac{\|f_l^\nu \circ f_l^\mu(h_{l-1}) - \tau_l\|_2^2}{2\beta} & (t \in \mathbb{E}) \\ \frac{\|f_l^\mu(h_{l-1}) + \epsilon - g_l^\mu \circ f_l^\nu(f_l^\mu(h_{l-1}) + \epsilon)\|_2^2}{2} & (t \in \mathbb{O}) \end{cases} \quad (37)$$

where $h_{l-1} \in \mathcal{X}_l$ is the feedforward activation from the layer $l-1$, $\tau_l \in \mathcal{X}_l$ is the target at the layer l , ϵ is a small Gaussian noise, and β is a hyper-parameter. We assumed \mathcal{X}_l and \mathcal{Z}_l are normed spaces.

When $g_l^\mu \circ \psi_l \circ f_l^\nu \circ f_l^\mu$ is bijective, Difference target propagation (DTP) is formulated as follows.

Definition A.3 (Difference Target Propagation). Suppose $g_l^\mu \circ \psi_l \circ f_l^\nu \circ f_l^\mu : \mathcal{X}_{l-1} \rightarrow \mathcal{W}_l$ is bijective. With two parameterized function spaces p_Θ and p_Ω , a training step of DTP is defined as follows. The search space is given by

$$\begin{aligned} \mathfrak{D}_l &= \{\mathbf{q}_l = (f_l^\nu, f_l^\mu, g_l^\nu, g_l^\mu) : \\ &\quad f_l^\nu \in p_\Theta, f_l^\mu = id, g_l^\mu \in p_\Omega, \Pi(\mathbf{q}_l) = 0\} \end{aligned} \quad (38)$$

where $\Pi : \mathfrak{D}_l \rightarrow \mathbb{R}_{\geq 0}$ is a *restrictor* given by

$$\begin{aligned} \Pi(\mathbf{q}_l) &= d_{P, \mathcal{X}_{l-1}}(f_l^\nu \circ g_l \circ f_l^*, \\ &\quad g_l^\mu \circ f_l^* + f_l^\mu - g_l^\mu \circ f_l). \end{aligned} \quad (39)$$

Note that $f_l^* = \psi_l \circ f_l$, and $\psi_l(h_l) = \tau_l$ is a shortcut as defined in Sec. 3. Here, d_{P, \mathcal{X}_l} a distance measure between two functions defined by

$$d_{P, \mathcal{X}_{l-1}}(\chi, \chi') = \int_{\mathcal{X}_{l-1}} d\lambda(x) \|\chi(x) - \chi'(x)\|_P \quad (40)$$

where χ and χ' are functions from \mathcal{X}_{l-1} to \mathcal{W}_l . Here, we assumed $(\mathcal{X}_{l-1}, \lambda)$ is a Lebesgue measurable space with a measure λ , the two input functions in Eq. (39) are measurable functions, and \mathcal{W}_l is a normed space with norm P . For example, L_2 norm is reasonable if \mathcal{W}_l is a real vector space. At time step t , the restricted search space is given, in the same form as TP, as follows:

$$\begin{aligned} \mathfrak{D}_l^{(t)}[\mathbf{q}^{(t)}] &= \left\{ \begin{aligned} &\{(f_l^\nu, id, g_l^\nu, g_l^\mu) \in \mathfrak{D}_l : f_l^\nu \in p_\Theta, g_l^\mu = p_{\omega_t}\} \quad (t \in \mathbb{E}) \\ &\{(f_l^\nu, id, g_l^\nu, g_l^\mu) \in \mathfrak{D}_l : f_l^\nu = p_{\theta_t}, g_l^\mu \in p_\Omega\} \quad (t \in \mathbb{O}) \end{aligned} \right. \end{aligned} \quad (41)$$

The objective function is given by Eq. (37).

DTP works deterministically because we have the following proposition.

Proposition A.1. The following search space $\bar{\mathfrak{D}}$ is *deterministic*, i.e., $\forall \mathbf{q}, \mathbf{q}' \in \bar{\mathfrak{D}} \mathbf{q} = \mathbf{q}'$ a.e.³, if functions p_1, p_2, p_3 and ψ_l are bijective:

$$\begin{aligned} \bar{\mathfrak{D}} &= \{\mathbf{q}_l = (f_l^\nu, f_l^\mu, g_l^\nu, g_l^\mu) \in \mathfrak{D}_l : \\ &\quad f_l^\nu = p_1, f_l^\mu = p_2, g_l^\mu = p_3, \Pi(\mathbf{q}_l) = 0\} \end{aligned} \quad (42)$$

³Given two quadruplets $\mathbf{q} = (f^\nu, f^\mu, g^\nu, g^\mu)$ and $\mathbf{q}' = (f'^\nu, f'^\mu, g'^\nu, g'^\mu)$, this means that $f^\nu = f'^\nu$, $f^\mu = f'^\mu$, $g^\nu = g'^\nu$ a.e., and $g^\mu = g'^\mu$. If we ignore function differences on zero-measure sets, this is equivalent to $|\bar{\mathfrak{D}}| = 1$. We call the space is deterministic because of this.

where Π is given by Eq. (39).

(Proof) From $\Pi(\mathbf{q}_l) = 0$, we have

$$f_l^\mu \circ g_l^\nu \circ g_l^\mu \circ f_l^* = g_l^\mu \circ f_l^* + f_l^\mu - g_l^\mu \circ f_l \quad \lambda\text{-a.e.} \quad (43)$$

Since there exists inverse functions $(f_l^\nu)^{-1}, (\psi_l)^{-1}, (g_l^\mu)^{-1}$ and $(f_l^\mu)^{-1}$, we have the following function that satisfies Eq. (43):

$$\begin{aligned} g_l^\nu &= (f_l^\mu)^{-1} \circ (g_l^\mu \circ f_l^* + f_l^\mu - g_l^\mu \circ f_l) \\ &\quad \circ (f_l^*)^{-1} \circ (g_l^\mu)^{-1} \\ &= (f_l^\mu)^{-1} \circ (id + f_l^\mu \circ (f_l^*)^{-1} \circ (g_l^\mu)^{-1} \\ &\quad - g_l^\mu \circ f_l \circ (f_l^*)^{-1} \circ (g_l^\mu)^{-1}) \\ &= (f_l^\mu)^{-1} \circ (id + (f_l^\nu)^{-1} \circ (\psi_l)^{-1} \circ (g_l^\mu)^{-1} \\ &\quad - g_l^\mu \circ (\psi_l)^{-1} \circ (g_l^\mu)^{-1}). \end{aligned} \quad (44)$$

This is the unique function that satisfies $\Pi(\mathbf{q}_l) = 0$ with exception of values on zero-measure sets because the inverse of a bijective function is unique. Thus, we have

$$\begin{aligned} \bar{\mathfrak{D}} &= \{\mathbf{q}_l = (f_l^\nu, f_l^\mu, g_l^\nu, g_l^\mu) : \\ &\quad f_l^\nu = p_1, f_l^\mu = p_2, g_l^\nu \in \mathfrak{G}, g_l^\mu = p_3\} \end{aligned} \quad (45)$$

where $\mathfrak{G} = \{g : g = \check{g}_l^\nu \lambda''\text{-a.e.}\}$, λ'' is a measure on \mathcal{W}_l , and

$$\begin{aligned} \check{g}_l^\nu &:= (f_l^\mu)^{-1} \circ (id + (f_l^\nu)^{-1} \circ (\psi_l)^{-1} \circ (g_l^\mu)^{-1} \\ &\quad - g_l^\mu \circ (\psi_l)^{-1} \circ (g_l^\mu)^{-1}). \end{aligned} \quad (46)$$

This shows that $\bar{\mathfrak{D}}$ is deterministic.

Practically, DTP and its variants often outperform TP because the restrictor Π is well designed to satisfy some requirements of learning as discussed in Sec. 3.5. However, as pointed out in recent studies, DTP is unstable if feedforward function is not injective. With our formulation, the instability is realized by that $\bar{\mathfrak{D}}$ becomes empty.

Proposition A.2. Suppose $p_1 \circ p_3 : \mathcal{X}_{l-1} \rightarrow \mathcal{X}_l$ is not injective, and p_2 and ψ_l are bijective for the search space $\bar{\mathfrak{D}}$ in Eq. (42). Suppose also $(\mathcal{X}_{l-1}, \lambda)$ and $(\mathcal{X}_l, \lambda')$ are Lebesgue measurable spaces. If there exists two subsets $O_1, O_2 \subset \mathcal{X}_{l-1}$ that satisfy

$$\lambda(O_1 \cap O_2) = 0, \quad (47)$$

$$\lambda'(p_1 \circ p_3(O_1) \cap p_1 \circ p_3(O_2)) > 0, \quad (48)$$

the search space is empty, i.e., $|\bar{\mathfrak{D}}| = 0$.

(Proof) Assume, for contradiction, that $|\bar{\mathfrak{D}}| > 0$. For $\mathbf{q}_l = (f_l^\nu, f_l^\mu, g_l^\nu, g_l^\mu) \in \bar{\mathfrak{D}}$, from $\Pi(\mathbf{q}_l) = 0$, we have

$$\begin{aligned} f_l^\mu \circ g_l^\nu \circ g_l^\mu \circ f_l^*(o_1) \\ = g_l^\mu \circ f_l^*(o_1) + f_l^\mu(o_1) - g_l^\mu \circ f_l(o_1) \quad \lambda\text{-a.e. } o_1 \in O_1 \end{aligned} \quad (49)$$

and

$$\begin{aligned} f_l^\mu \circ g_l^\nu \circ g_l^\mu \circ f_l^*(o_2) \\ = g_l^\mu \circ f_l^*(o_2) + f_l^\mu(o_2) - g_l^\mu \circ f_l(o_2) \quad \lambda\text{-a.e. } o_2 \in O_2. \end{aligned} \quad (50)$$

From $\lambda'(p_1 \circ p_3(O_1) \cap p_1 \circ p_3(O_2)) > 0$, we have a positive-measure pair set

$$Q = \{(o_1, o_2) : p_1 \circ p_3(o_1) = p_1 \circ p_3(o_2)\} \quad (51)$$

where $Q \subset O_1 \times O_2$ and each of $(o_1, o_2) \in Q$ satisfies

$$\begin{aligned} f_l^\mu \circ g_l^\nu \circ g_l^\mu \circ f_l^*(o_1) &= f_l^\mu \circ g_l^\nu \circ g_l^\mu \circ \psi_l \circ p_1 \circ p_3(o_1) \\ &= f_l^\mu \circ g_l^\nu \circ g_l^\mu \circ \psi_l \circ p_1 \circ p_3(o_2) \\ &= f_l^\mu \circ g_l^\nu \circ g_l^\mu \circ f_l^*(o_2). \end{aligned} \quad (52)$$

Further, the pairs also satisfies

$$\begin{aligned} g_l^\mu \circ f_l^*(o_1) + f_l^\mu(o_1) - g_l^\mu \circ f_l(o_1) \\ = g_l^\mu \circ f_l^*(o_2) + f_l^\mu(o_2) - g_l^\mu \circ f_l(o_2). \end{aligned} \quad (53)$$

From Eqs. (49), (50), (52), and (53), we have

$$\begin{aligned} g_l^\mu \circ f_l^*(o_2) + f_l^\mu(o_1) - g_l^\mu \circ f_l(o_2) \\ = g_l^\mu \circ f_l^*(o_2) + f_l^\mu(o_2) - g_l^\mu \circ f_l(o_2) \end{aligned} \quad (54)$$

and thus $f_l^\mu(o_1) = f_l^\mu(o_2)$ follows for pairs in Q . Since f_l^μ is bijective, the measure of $\{o_1 : (o_1, o_2) \in Q, o_1 = o_2\}$ is positive. This contradicts to the assumption of $\lambda(O_1 \cap O_2) = 0$.

This raises a question: How is DTP working with non injective feedforward function? The answer is that DTP applies the restrictor Π at each time step by relaxing the Eq. (40) as

$$\begin{aligned} d_{P, A_t}(\chi|_{A_t}, \chi'|_{A_t}) \\ := \int_{A_t} d\kappa(x) \|\chi|_{A_t}(x) - \chi'|_{A_t}(x)\|_P. \end{aligned} \quad (55)$$

Here, $A_t \subset \mathcal{X}_{l-1}$ is a measurable subset such that $(g_l^\mu \circ \psi_l \circ f_l^\nu \circ f_l^\mu)|_{A_t} : A_t \rightarrow \text{Im}A_t$ is bijective, where the notation $\chi|_A$ denotes restriction⁴ of χ to A . Note that κ is a measure on A_t ⁵. The following gives the formulation.

Definition A.4 (DTP with non injective functions). A training step of DTP is defined as follows. With two parameterized function spaces p_Θ and p_Ω , the search space is given by

$$\begin{aligned} \mathfrak{D}_l &= \{(f_l^\nu, f_l^\mu, g_l^\nu, g_l^\mu) : \\ &\quad f_l^\nu \in p_\Theta, f_l^\mu = id, \\ &\quad g_l^\nu \in \{g : \mathcal{W}_l \rightarrow \mathcal{X}_{l-1}\}, g_l^\mu \in p_\Omega\}. \end{aligned} \quad (56)$$

At time step t , a *local restrictor* Π_t is applied to determine g_l^μ as follows:

$$\begin{aligned} \mathfrak{D}_l^{(t)}[\mathbf{q}^{(t)}] \\ = \begin{cases} \{\mathbf{q}_l = (f_l^\nu, id, g_l^\nu, g_l^\mu) \in \mathfrak{D}_l : \\ \quad f_l^\nu \in p_\Theta, g_l^\mu = p_{\omega_t}, \Pi_t(\mathbf{q}_l) = 0\} & (t \in \mathbb{E}) \\ \{\mathbf{q}_l = (f_l^\nu, id, g_l^\nu, g_l^\mu) \in \mathfrak{D}_l : \\ \quad f_l^\nu = p_{\theta_t}, g_l^\mu \in p_\Omega \Pi_t(\mathbf{q}_l) = 0\} & (t \in \mathbb{O}) \end{cases} \end{aligned} \quad (57)$$

⁴We also restrict the codomain of χ to $\text{Im}A$.

⁵This may not be the same measure as λ on \mathcal{X}_l , even if A_t is a zero-measure set with the measure λ , $\kappa(A_t)$ may be positive.

where Π_t is a restrictor given by

$$\begin{aligned} \Pi_t(\mathbf{q}) = d_{P,A_t} &((f_l^\mu \circ g_l \circ f_l^*)|_{A_t}, \\ &(g_l^\mu \circ f_l^*)|_{A_t} + f_l^\mu|_{A_t} - (g_l^\mu \circ f_l)|_{A_t}) \end{aligned} \quad (58)$$

with a subset $A_t \subset \mathcal{X}_{l-1}$ such that $(g_l^\mu \circ \psi_l \circ f_l^\nu \circ f_l^\mu)|_{A_t}$ is bijective.

If A_t exists, we see with this definition that

$$\begin{aligned} \bar{\mathfrak{D}}_l^{(t)} := \{\mathbf{q}_l = (f_l^\nu, id, g_l^\nu, g_l^\mu) \in \mathfrak{D}_l : \\ f_l^\nu = p_{\theta_t}, g_l^\mu = p_{\omega_t}, \Pi_t(\mathbf{q}_l) = 0\} \end{aligned} \quad (59)$$

becomes not empty. More specifically, similar to Prop. A.1, we obtain

$$\begin{aligned} \check{g}_l^{\nu(t)} = &(f_l^\mu|_{A_t})^{-1} \circ (id \\ &+ (f_l^\nu|_{B_t})^{-1} \circ (\psi_l|_{C_t})^{-1} \circ (g_l^\mu|_{D_t})^{-1} \\ &- g_l^\mu|_{D_t} \circ (\psi_l|_{C_t})^{-1} \circ (g_l^\mu|_{D_t})^{-1}) \end{aligned} \quad (60)$$

where $B_t = \text{Im } f_l^\mu|_{A_t} \subset \mathcal{Z}_l$, $C_t = \text{Im } f_l^\nu|_{B_t} \subset \mathcal{X}_l$, and $D_t = \text{Im } \psi_l|_{C_t} \subset \mathcal{X}_l$. Note that the domain of $\check{g}_l^{\nu(t)}$ is $E_t = \text{Im } g_l^\mu|_{D_t} \subset \mathcal{W}_l$. Thus, we have

$$\begin{aligned} \bar{\mathfrak{D}}_l^{(t)} = \{\mathbf{q}_l = (f_l^\nu, id, g_l^\nu, g_l^\mu) : \\ f_l^\nu = p_{\theta_t}, g_l^\nu \in \mathfrak{G}_t, g_l^\mu = p_{\omega_t}\} \end{aligned} \quad (61)$$

where

$$\mathfrak{G}_t = \{\check{g} \in \{\mathcal{W}_l \rightarrow \mathcal{X}_l\} : g|_{E_t} = \check{g}_l^{\nu(t)}\}, \quad (62)$$

that is, a function in \mathfrak{G}_t is an extension of $\check{g}_l^{\nu(t)}$ from E_t to \mathcal{W}_t . At each time step t in DTP, there must be one function quadruplet implicitly chosen from $\bar{\mathfrak{D}}_l^{(t)}$. Intuitive understanding of this is that DTP determines g_l^ν by only seeing a subset $A_t \subset \mathcal{X}_{l-1}$ where every function becomes bijective.

The subset A_t is determined depends on the input sequence for training. In online learning, where inputs are given point-wise, A_t always exists. The following proposition is trivial, but helps to understand what DTP does.

Proposition A.3. Given an input⁶ of online learning $x_t \in \mathcal{X}_{l-1}$ at time t to layer l , there exists $A_t \supset \{x_t\}$ that makes $(g_l^\mu \circ \psi_l \circ f_l^\nu \circ f_l^\mu)|_{A_t}$ bijective.

(Proof) Let $X_t = \{x_t\}$. Clearly, $A_t = X_t$ makes all functions $f_l^\mu|_{A_t}$, $f_l^\nu|_{B_t}$, $g_l^\mu|_{C_t}$, and $g_l^\nu|_{D_t}$ bijective because we have $|B_t| = |C_t| = |D_t| = 1$.

Piratically, in mini-batch learning, the input is given by $X_t = \{x_{t,i}\}_{i=1}^N \subset \mathcal{X}_{l-1}$. Under some proper assumptions on $\mathcal{X}_{l-1}, \mathcal{X}_l$ (such as both of them are dense vector spaces whose dimension is large enough), $(g_l^\mu \circ \psi_l \circ f_l^\nu \circ f_l^\mu)|_{A_t}$ becomes bijective with $A_t = X_t$ with probability of 1.0 because X_t is a finite zero-measure set. This shows how DTP is working with non injective feedforward function.

⁶The input to layer l is the activation h_{l-1} , but we use notation x_t for simplicity.

From above, we obtain a sequence of the restricted spaces $\bar{\mathfrak{D}}_l^{(0)}, \bar{\mathfrak{D}}_l^{(1)}, \bar{\mathfrak{D}}_l^{(2)}, \dots$, from each of which DTP implicitly chooses one function quadruplet $\mathbf{q} \in \bar{\mathfrak{D}}_l^{(t)}$ at each time step t . Our interest lies in whether there exists a common solution over t , i.e., whether $\exists t^\dagger \geq 0$ s.t. $|\bigcap_{t=t^\dagger}^\infty \bar{\mathfrak{D}}_l^{(t)}| > 0$. The time step t^\dagger is a large enough number to see the final phase of training where f_l^μ, f_l^ν and g_l^μ have converged⁷.

Here, we consider online learning where $X_t = \{x_t\}$ is given as an input at time t , and fix f_l^μ, f_l^ν and g_l^μ to analyze g_l^ν . The following proposition is also trivial, but shows there often exists global g_l^ν .

Proposition A.4. Let $X_t = \{x_t\}$ ($t = 0, 1, 2, \dots$) be an input sequence for online training, and

$$\begin{aligned} \bar{\mathfrak{D}}_l^{(t)} = \{\mathbf{q}_l = (f_l^\nu, f_l^\mu, g_l^\nu, g_l^\mu) \in \mathfrak{D}_l : \\ f_l^\nu = p_1, f_l^\mu = p_2, g_l^\mu = p_3, \Pi_t(\mathbf{q}_l) = 0\} \end{aligned} \quad (63)$$

be the restricted search space at time step t where $A_t = X_t$ is used to define Π_t . With $A = \{x_t\}_{t=1}^\infty$, if $(g_l^\mu \circ \psi_l \circ f_l^\nu \circ f_l^\mu)|_A$ is bijective, $\bigcap_{t=1}^\infty \bar{\mathfrak{D}}_l^{(t)}$ is not empty.

(Proof) Because A is a finite or countably infinite set, there exists a common discrete measure for all A_t and A that satisfies

$$\begin{aligned} \sum_{t=1}^\infty \Pi_t(\mathbf{q}_l) = \sum_{t=1}^\infty d_{P,A_t} &((f_l^\mu \circ g_l \circ f_l^*)|_{A_t}, \\ &(g_l^\mu \circ f_l^*)|_{A_t} + f_l^\mu|_{A_t} - (g_l^\mu \circ f_l)|_{A_t}) \\ = d_{P,A} &((f_l^\mu \circ g_l \circ f_l^*)|_A, \\ &(g_l^\mu \circ f_l^*)|_A + f_l^\mu|_A - (g_l^\mu \circ f_l)|_A). \end{aligned} \quad (64)$$

Replacing A_t by A in Eq. (60), we have a quadruplet \mathbf{q}_l that satisfies $\Pi_t(\mathbf{q}_l) = 0$ for all t , and thus $\bigcap_{t=0}^\infty \bar{\mathfrak{D}}_l^{(t)}$ is not empty.

Again, since inputs for training are given sequentially, and a training set is finite or countably infinite, $(g_l^\mu \circ \psi_l \circ f_l^\nu \circ f_l^\mu)|_A$ often becomes bijective under proper assumptions. This is the reason why DTP is applicable even if feedforward function is not injective.

However, a non-injective feedforward function may lead to non-continuous feedback function in DTP. More specifically, the obtained \check{g}_l^ν of $\mathbf{q}_l = (f_l^\nu, f_l^\mu, \check{g}_l^\nu, g_l^\mu) \in \bigcap_{t=0}^\infty \bar{\mathfrak{D}}_l^{(t)}$ may be non-continuous even if $f_l^\nu, f_l^\mu, g_l^\mu$, and ψ_l are continuous. Note that if $f_l^\nu, f_l^\mu, g_l^\mu$, and ψ_l are bijective and continuous, from Eq. (46), there exists continuous \check{g}_l^ν , because the inverse of a continuous bijective function is continuous. Therefore, the feedback non-continuity is caused by the feedforward non-injectiveness. The following small extreme examples help to imagine the shape of feedback functions in DTP.

Example 1. The first example is on the one dimensional real space \mathbb{R} . Suppose $f_l^\mu(x) = x$, $f_l^\nu(x) = \frac{1}{2}(x^3 - 3x)$, $g_l^\mu(x) = x$, and inputs for training are given by $x_t = (-1)^t(1 + (t + 1)^{-1})$ for $t = 0, 1, 2, \dots$. There is no continuous function

⁷We assumed the convergence of these three functions to analyze g_l^ν . In general, they may oscillate.

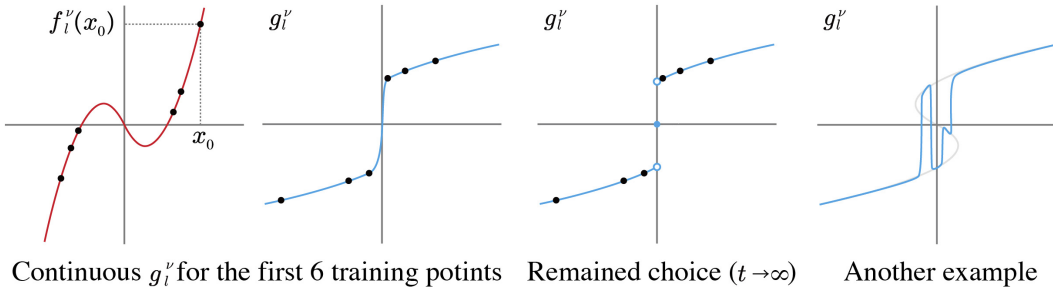


Figure 4: Example 1.

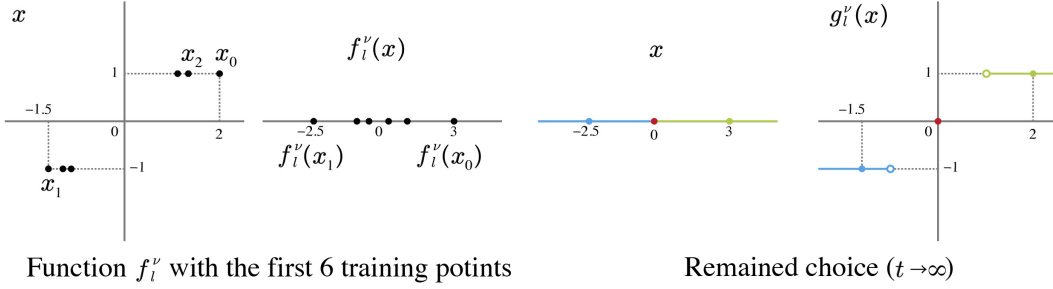


Figure 5: Example 2.

quadruplet remains in $\bigcap_{t=0}^{\infty} \bar{\mathcal{D}}_l^{(t)}$. Figure 4 illustrates one of remaining choices for g_l^ν of $q \in \bigcap_{t=0}^{\infty} \bar{\mathcal{D}}_l^{(t)}$ given by

$$g_l^\nu(x) = \begin{cases} (x + (x^2 - 1)^{\frac{1}{2}})^{\frac{1}{3}} \\ \quad + (x - (x^2 - 1)^{\frac{1}{2}})^{\frac{1}{3}} & (|x| \geq 1) \\ \cos(\arccos(\frac{x}{3})) & (0 < x < 1) \\ \cos(\arccos(\frac{x+2\pi}{3})) & (-1 < x < 0) \\ 0 & (x = 0) \end{cases}. \quad (65)$$

This is not continuous at 0. In the figure, we also show another example of g_l^ν where training inputs are distributed around $x = 0$. This is an extreme case but DTP may propagate targets in similar ways.

Example 2. The second example is from \mathbb{R}^2 to \mathbb{R} . Suppose $f_l^\mu = id$, $f_l^\nu(x^{(1)}, x^{(2)}) = x^{(1)} + x^{(2)}$ for $(x^{(1)}, x^{(2)}) \in \mathbb{R}^2$, $g_l^\mu = id$, and inputs are given by $(x_t^{(1)}, x_t^{(2)}) = ((-1)^t(1 + (t+1)^{-1}), (-1)^t)$ for $t = 0, 1, 2, \dots$. There is no continuous function quadruplet remains in $\bigcap_{t=0}^{\infty} \bar{\mathcal{D}}_l^{(t)}$. Figure 5 illustrates $g_l^\nu : \mathbb{R} \rightarrow \mathbb{R}^2$ given by

$$g_l^\nu(x) = \begin{cases} (x - 1, 1) & (x > 0) \\ (x + 1, -1) & (x < 0) \\ (0, 0) & (x = 0) \end{cases}. \quad (66)$$

This shows that feedforward function with dimension reduction may also cause non-continuous feedback in DTP.

Finally, we discuss pros and cons of updating parameters of g_l^μ with a reconstruction loss. The advantages are clear. If the feedforward function is bijective, g_l^μ approaches to the inverse of f_l^ν and this makes better targets. Note that

\check{g}_l^ν approaches the inverse of f_l^μ , which is assumed to be the identity function in DTP. Recent studies have shown that modifying reconstruction loss significantly improve the performance of DTP (Frenkel, Lefebvre, and Bol 2021; Meulemans et al. 2020) by propagating information from some top layers ($l' > l$) to l . These techniques contribute to stabilizing training.

A disadvantage we found here is that updating g_l^μ potentially makes it difficult to find continuous g_l^ν . As we can image from the two extreme examples, the feedback function easily becomes non-Lipschitz continuous function, and may approach to non-continuous function. Figure 6 considers a binary classification problem for discussion. At the beginning of training, f_{l-1}^μ is a randomly chosen function, and thus the minimum radius that covers the inputs $A = \{x_t\}_{t=0}^{\infty} \subset \mathcal{X}_{l-1}$ for layer l is large (these inputs are the activations from $(l-1)$ -th layer). After some training steps, f_{l-1} often approaches to non-injective function $f_{l-1}^* : \mathcal{X}_{l-2} \rightarrow \{a_{\text{neg}}, a_{\text{pos}}\}$, which maps all points in \mathcal{X}_{l-2} into two points $a_{\text{neg}}, a_{\text{pos}} \in \mathcal{X}_{l-1}$, where $a_{\text{neg}}, a_{\text{pos}}$ represent the positive class and the negative class, respectively⁸. In this case, we only have points around a_{pos} and a_{neg} to compute reconstruction loss to update g_l^μ . According to Prop. A.2., this potentially narrows the search space because the overlap of two images $g_l^\mu(O_1) \cap g_l^\mu(O_2)$ of two disjoint sets $O_1, O_2 \subset \mathcal{X}_l$ tends to increase around a_{pos} and/or a_{neg} by updating g_l^μ . Unfortunately, adding small ϵ to each x_t to compute reconstruction loss does not fully resolves this prob-

⁸This assumption is strong, but a C -class classification problem can be seen as a problem to find a non-injective mapping from inputs to $\{1, 2, \dots, C\}$. Thus, forward functions often approaches to some non-injective functions to some extent.

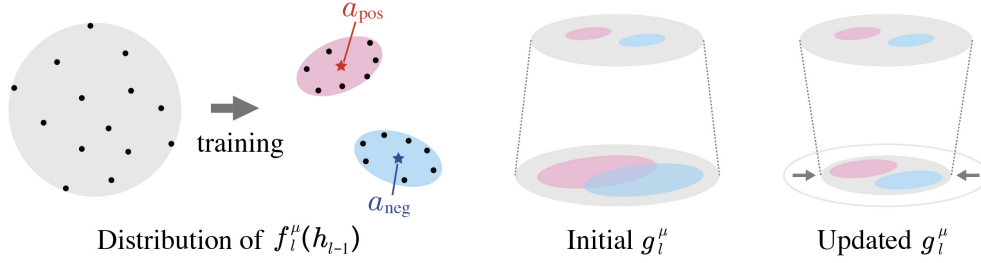


Figure 6: Distribution of $f_l^\mu(h_{l-1})$ before and after training f_{l-1}^ν and updates of g_l^μ .

lem. Updating f_l^μ also has similar effect, but this would be unavoidable.

From this discussion we reach to an idea to slowdown updates of feedback weights. For example, in Eq. (37), we can replace \mathbb{O} and \mathbb{E} by $\mathbb{N}_n := \{nk : k \in \mathbb{N}\} = \{0, n, 2n, 3n, \dots\}$ and $\mathbb{N}_n^c = \mathbb{N} \setminus \mathbb{N}_n$, respectively, with $n > 2$, as follows:

$$\mathcal{O}_l^{(t)} = \begin{cases} \frac{\|f_l^\nu(h_{l-1}) - \tau_l\|_2^2}{2\beta} & (t \in \mathbb{N}_n^c) \\ \frac{\|h_{l-1} + \epsilon - g_l^\mu \circ f_l^\nu(h_{l-1} + \epsilon)\|_2^2}{2} & (t \in \mathbb{N}_n) \end{cases}. \quad (67)$$

FW-DTP is the algorithm obtained from $n \rightarrow \infty$, where there exists reconstruction loss, but it will never be used.

Biological plausibility need to be discussed carefully, because we decomposed encoder and decoder into two functions respectively. The main idea of TP is to parameterize f_l^ν and g_l^μ in the same way, e.g., $f_l^\nu(x) = \sigma(Wx)$ and $g_l^\mu(x) = \sigma(\Omega x)$ where W, Ω are learnable matrices and σ is an activation function. However, with our formulation, the decoder $g_l = g_l^\nu \circ g_l^\mu$ has $g_l^\nu \in \mathfrak{G}_l$, in contrast to $f_l^\mu = id$ for the encoder. FW-DTP did not resolve this asymmetry, but it has another symmetry that (f_l^μ, g_l^μ) are fixed and (f_l^ν, g_l^ν) are determined by a parameter θ .

This would help to explore new variants of DTP. In this paper, we fixed $f_l^\mu = id$ to fairly compare FW-DTP with TP and DTP variants. However, in future work, designing new search space, the the following generalized DTP is interesting:

Definition A.5 Generalized DTP (GDTP). Let p_Θ be a parameterized function space. GDTP uses the search space of

$$\begin{aligned} \mathfrak{D}_l = \{q_l = (h_l, f_l^\nu, f_l^\mu, g_l^\nu, g_l^\mu) : \\ h_l \in p_\Theta, f_l^\mu = \{r_1\}, f_l^\nu \in \{\mathcal{Z}_l \rightarrow \mathcal{X}_{l+1}\}, \\ g_l^\mu = \{r_2\}, g_l^\nu \in \{\mathcal{W}_l \rightarrow \mathcal{X}_l\}, \Pi^*(q_l) = 0\} \end{aligned} \quad (68)$$

where h_l is parameterized, f_l^μ, g_l^μ are fixed functions r_1 and r_2 , and Π^* is a restrictor that determines f_l^μ and g_l^ν .

When $f_l^\nu = h_l$ and $f_l^\mu = id$, GDTP reduces DTP, but for biological plausibility, (1) f_l^ν and g_l^ν should have the same form, (2) r_1 and r_2 should have the same form, and (3) Π^* should be symmetric to (f_l^ν, g_l^ν) and (f_l^μ, g_l^μ) . We left this for future work.

B Proof of Eq. (16) \Leftrightarrow Eq. (17)

Let $\mathcal{N}(0, \mathbb{I})$ be the standard Gaussian distribution. We have

$$\begin{aligned} \mathbb{E}_{\epsilon \sim \mathcal{N}(0, \mathbb{I})} [\epsilon^\top J_{f_l} J_{g_l} \epsilon] &= \mathbb{E}_{\epsilon \sim \mathcal{N}(0, \mathbb{I})} [\text{tr}(\epsilon \epsilon^\top J_{f_l} J_{g_l})] \\ &= \text{tr}(\mathbb{E}_{\epsilon \sim \mathcal{N}(0, \mathbb{I})} [\epsilon \epsilon^\top J_{f_l} J_{g_l}]) \\ &= \text{tr}(\mathbb{E}_{\epsilon \sim \mathcal{N}(0, \mathbb{I})} [\epsilon \epsilon^\top]) J_{f_l} J_{g_l}) \\ &= \text{tr}(\mathbb{I} J_{f_l} J_{g_l}) \\ &= \text{tr}(J_{f_l} J_{g_l}) \end{aligned}$$

and thus we have

$$\mathbb{E}_{\epsilon \sim \mathcal{N}(0, \mathbb{I})} [\epsilon^\top J_{f_l} J_{g_l} \epsilon] \geq 0 \Leftrightarrow \text{tr}(J_{f_l} J_{g_l}) \geq 0. \quad (69)$$

C Necessity and Effectiveness of Batch Normalization in DTP and FW-DTP

In this section, we investigate the necessity and effectiveness of batch normalization (BN) (Ioffe and Szegedy 2015) in DTP-derived methods. First, we overview BN. Let $\mathcal{B} = \{h_i\}_{i=1}^M$ be a mini-batch of activation, where M is the mini-batch size and $h_i = (h_i^{(1)}, \dots, h_i^{(D)})$ is a D -dimensional activation vector. The normalized activation \hat{h}_i is defined by

$$\hat{h}_i^{(d)} = \frac{h_i^{(d)} - \mu_{\mathcal{B}}^{(d)}}{\sigma_{\mathcal{B}}^{(d)}} \quad (70)$$

where

$$\mu_{\mathcal{B}}^{(d)} = \frac{1}{M} \sum_{j=1}^M h_j^{(d)}, \quad \sigma_{\mathcal{B}}^{(d)} = \frac{1}{M} \sum_{j=1}^M (h_j^{(d)} - \mu_{\mathcal{B}}^{(d)})^2 \quad (71)$$

for $d = 1, \dots, D$. The batch normalization function $\text{BN}_{\gamma, \delta}(\cdot)$ is defined by

$$\text{BN}_{\gamma, \delta}(h_i) := \gamma \hat{h}_i + \delta \quad (72)$$

where γ and δ are learnable parameters.

In FW-DTP, the weak condition expressed in Eq. (16) between the feedforward and feedback networks is acquired in the learning process; however, in the early stage of the learning process, the target τ_l propagated by the feedback network deviates significantly from the activation h_l if BN is not applied, which destabilizes the learning process and makes the test performance worse. BN resolves this optimization problem. We fix the parameters γ, δ and use

Table 4: Test error (%) obtained with and without batch normalization on four image classification datasets reported with the mean and standard deviation over five different seeds. The best results are marked in bold.

METHODS	MNIST	F-MNIST	CIFAR-10	CIFAR-100
DTP w/o BN	2.77 \pm 0.10	11.77 \pm 0.16	52.01 \pm 0.80	77.11 \pm 0.20
DTP w BN	3.51 \pm 0.17	12.74 \pm 0.22	52.58 \pm 0.43	77.36 \pm 0.31
FW-DTP w/o BN	2.86 \pm 0.14	13.49 \pm 0.60	51.22 \pm 2.03	75.38\pm0.34
FW-DTP w BN	2.76\pm0.10	11.76\pm0.37	48.97\pm0.32	76.76 \pm 0.45

$\gamma = 1$, $\delta = 0$ for all hidden layers in both of the feed-forward and feedback networks. Using this fixed BN, the mean of each dimension of the targets computed according to Eq. (8) are also 0, so h_l and τ_l are relatively close to each other from the beginning of the learning process. Note that a constant other than 0 can be used as the fixed value of γ , while we chose 0 for the simplicity and symmetry with respect to origin.

The test performances obtained by DTP and FW-DTP with and without BN are shown in Table 4. In FW-DTP, the test performances are considerably improved by using BN for all datasets except CIFAR-100. On the other hand, in DTP, the test performances are slightly worse with BN than without for all datasets. This suggests that fixing the mean and variance has a negative effect; since the feedback network is trained in parallel in DTP, the target τ_l and the feedforward activation h_l are close even without BN.

From these results, it can be concluded that FW-DTP without BN can achieve almost the same level of test performance as DTP, and it performs even better when BN is used; however, BN is not so effective for DTP.

D Connection between FW-DTP and DTP

In this section, we discuss the connection between FW-DTP and DTP in terms of learning rate for feedback network α_b . If α_b is set to zero in DTP, the feedback weights are not updated, so the algorithm becomes the same as FW-DTP. What then is the behavior of the test performance when α_b is asymptotically approaching zero?

Figure 7 shows the result on CIFAR-10. The values of hyperparameters other than α_b are the same as those of DTP used in 4.2 and BN is not used in the activation functions. If α_b becomes close to 0, it asymptotically approaches FW-DTP (without BN). At $\alpha_b = 0$, the test accuracy is actually 48.80 ± 2.06 , indicating that DTP converges to FW-DTP. As the figure shows, the test accuracy reaches a local maximum around $\alpha_b = 6 \times 10^{-3}$, and the accuracy decreases as α_b is reduced. Interestingly, the test accuracy begins to increase from around $\alpha_b = 3 \times 10^{-5}$, and finally, the test accuracy is on the same level as the local maximum around $\alpha_b = 6 \times 10^{-3}$ with a sufficiently small α_b . Note that FW-DTP is slightly destabilized and the standard deviation is increased because BN is not used.

This result indicates that α_b , which cannot make the feedback network a precise inverse of the feedforward network but is large enough to add some perturbation to the feedback weights, adds noise to the feedback weights and degrades

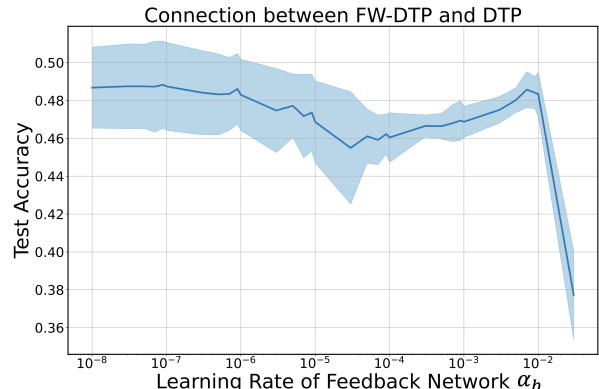


Figure 7: The connection between FW-DTP and DTP by adjusting the learning rate for the feedback network on CIFAR-10. Test accuracy are shown with the mean and standard deviation over ten different seeds. The values of hyperparameters other than the learning rate of feedback network are the same as those used in 4.2.

the test performance. On the other hand, if α_b is sufficiently small, the update of feedback weights can be ignored, *i.e.*, DTP can approximate FW-DTP, thus improving the test performance.

E Evaluation with Large and Small Network

In this section, we discuss the scalability of FW-DTP. Tables 5 and 6 report accuracy of BP, DTP, and FW-DTP on CIFAR 10 with varying numbers of layers and hidden units, respectively. We see that FW-DTP consistently outperforms DTP. However, the performance gap from BP increases as the size of network increases. This shows a limitation of FW-DTP. To deal with the scalability problem, some feedback connections from the top layer as proposed in direct feedback alignment (Nøkland 2016; Crafton et al. 2019) and improved target propagation (Meulemans et al. 2020; Ernoult et al. 2022) would be needed.

F Comparison of Algorithms

Table 7 summarizes characteristics of backpropagation (BP), feedback alignment (FA), direct feedback alignment (DFA) (Nøkland 2016), target propagation (TP), difference target propagation (DTP), and fixed-weight difference target propagation (FW-DTP). In terms of biological plausibility, all algorithms except of BP resolves the weight transport

Table 5: Error rate against the number of layers on CIFAR 10. The number of hidden units is 1024.

# OF LAYERS	5	6	7	8	9
BP	48.02 \pm 1.39	46.71 \pm 0.70	45.24 \pm 0.54	45.34 \pm 0.28	46.78 \pm 3.63
DTP	51.66 \pm 0.85	52.48 \pm 0.52	51.08 \pm 0.69	51.59 \pm 0.57	52.03 \pm 0.64
FW-DTP	49.47\pm0.28	50.06\pm0.53	50.54\pm0.49	50.50\pm0.44	50.51\pm0.10

Table 6: Error rate against the number of hidden units on CIFAR 10. The number of layers is 4.

# OF HIDDEN UNITS	64	128	256	512	1024	1536	2048
BP	52.50 \pm 0.41	51.02 \pm 0.51	50.05 \pm 0.41	49.58 \pm 0.93	46.43 \pm 1.59	44.45 \pm 0.35	43.88 \pm 0.69
DTP	55.63 \pm 0.21	54.34 \pm 0.34	53.05 \pm 0.35	52.14 \pm 0.71	51.91 \pm 0.42	52.77 \pm 0.86	52.39 \pm 0.50
FW-DTP	53.96\pm0.51	51.86\pm0.20	50.53\pm0.74	49.42\pm0.42	49.11\pm0.11	48.92\pm0.25	48.77\pm0.35

Table 7: Comparison of characteristics.

	BP	FA	DFA	TP	DTP	FW-DTP
No weight transport		✓	✓	✓	✓	✓
Local error signals			✓	✓	✓	✓
Function symmetry				✓	✓	✓
Fixed-feedback weights		✓	✓			✓

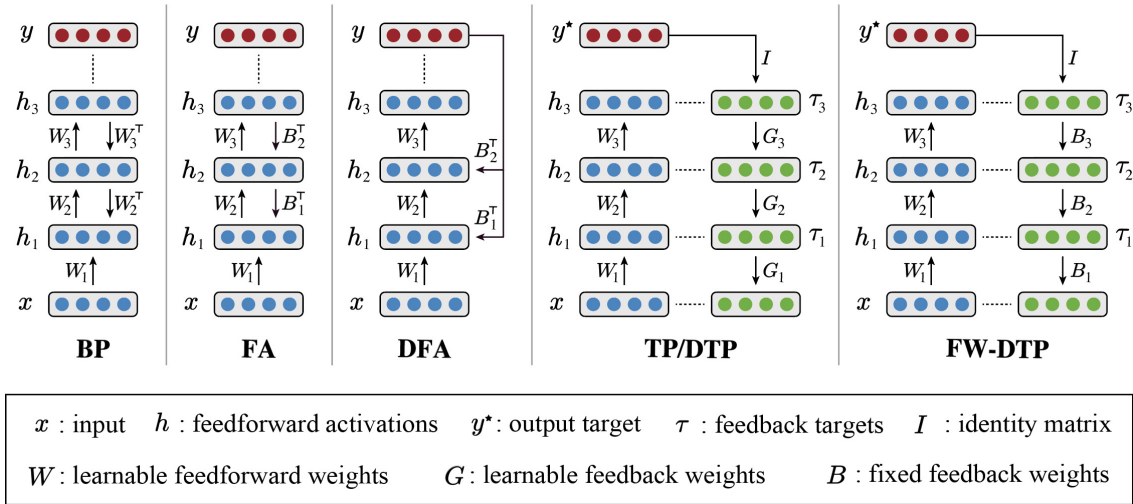


Figure 8: Comparison of propagation configurations.

problem. The error signals are local with DFA and all TP algorithms and this helps local (layer-wise) learning. TP algorithms can have the same function on the feedforward and feedback paths. Fixed feedback weights are used with FA, DFA, and FW-DTP.

Figure 8 compares propagation configurations of these algorithms. We see that FW-DTP propagates signals in a different way from FA while they commonly fix the feedback weights.

G Detailed Settings of Experiments

This section reports the detailed settings of the experiments in Section 4.

Algorithms. We first explain the exact algorithm of FW-DTP, DTP, DRL and L-DRL in Algorithms 1-4. For DTP, DRL and L-DRL, training is start with 1 epoch of feed-back weights training, then feedforward weights and feed-back weights are trained altogether with N_b feedback weight updates per batch; however, FW-DTP has no pre-training of feedback weights since it completely fixes the feedback

Algorithm 1: Fixed-Weight Difference Target Propagation (FW-DTP).

Hyperparameters: Learning Rate α_f , Stepsize β
Requires: Dataset D , Loss \mathcal{L} , Epochs N , Encoder f_l parameterized with W_l ($l = 1 \dots L$), Decoder g_l parameterized with fixed B_l ($l = 1 \dots L$)

Train the feedforward network:

```

for  $i = 1$  to  $N$  do
  for all  $(x, y) \in D$  do
     $h_0 = x$ 
    for  $l = 1$  to  $L$  do
       $h_l = f_l(h_{l-1})$ 
    Compute targets:
     $\tau_L = h_L - \beta \nabla_{h_L} \mathcal{L}(h_L, y)$ 
    for  $l = L - 1$  to  $1$  do
       $\tau_l = g_{l+1}(\tau_{l+1}) + h_l - g_{l+1}(h_{l+1})$ 
    Update the forward weights:
    for  $l = 1$  to  $L$  do
       $L_l = \|\tau_l - h_l\|_2^2$ 
       $W_l \leftarrow W_l - \alpha_f \nabla_{W_l} L_l$ 

```

weights. For all methods, the encoder f_l is parameterized as $f_l(h_{l-1}) = \sigma_l(W_l h_{l-1})$, where the non-linear activation function σ_l is a hyperbolic tangent function for DTP, DRL and L-DRL. For FW-DTP, the activation function $\sigma_l(h_{l-1})$ is $\text{BN}_{1,0}(\tanh(h_{l-1}))$ as explained in Appendix C. We chose the hyperbolic tangent function because it gave the best experimental results as consistently reported in the previous research (Lee et al. 2015; Bartunov et al. 2018; Meulemans et al. 2020). The decoder g_l is also parameterized as $g_l(\tau_l) = \sigma_l(\Omega_l \tau_l)$, where the activation function σ_l is the same function as the encoder’s activation function and for FW-DTP, $\Omega_l = B_l$ is a fixed random matrix. Note that Algorithms 1-4 show the case of the batch size is 1 for clarity.

Architectures. We used a stack of fully connected layers and a softmax layer as the network architecture for all methods and datasets. More detailed architectures used for each dataset are shown below:

- For MNIST: 5 fully connected layers with 256 hidden units + 1 output softmax layer with 10 units.
- For Fashion-MNIST: 5 fully connected layers with 256 hidden units + 1 output softmax layer with 10 units.
- For CIFAR-10: 3 fully connected layers with 1024 hidden units + 1 output softmax layer with 10 units.
- For CIFAR-100: 3 fully connected layers with 1024 hidden units + 1 output softmax layer with 100 units.

These architectures are reported as the architectures suited to DTP in the previous research (Bartunov et al. 2018). The reduced architectures whose number of learnable parameters are halved from the architectures above were used in 4.2, and their details are shown below:

- For MNIST: 5 fully connected layers with 164 hidden units + 1 output softmax layer with 10 units.

Algorithm 2: Difference Target Propagation (DTP) (Lee et al. 2015) with the original reconstruction loss.

Hyperparameters: Learning Rate α_f , α_b , Stepsize β , Feedback Update Frequency N_b , Standard Deviation σ

Requires: Dataset D , Loss \mathcal{L} , Epochs N , Encoder f_l parameterized with W_l ($l = 1 \dots L$), Decoder g_l parameterized with Ω_l ($l = 1 \dots L$)

Pre-train only feedback network:

```

for all  $(x, y) \in D$  do
   $h_0 = x$ 
  for  $l = 1$  to  $L$  do
     $h_l = f_l(h_{l-1})$ 
  Update the feedback weights:
  for  $j = 1$  to  $N_b$  do
    for  $l = 1$  to  $L$  do
       $r_l = h_l + \epsilon$ ,  $\epsilon \sim N(0, \sigma I)$ 
       $r_{l+1} = f_{l+1}(r_l)$ 
       $r_l^{rec} = g_{l+1}(r_{l+1})$ 
       $L'_l = \|r_l^{rec} - r_l\|_2^2$ 
       $\Omega_l \leftarrow \Omega_l - \alpha_b \nabla_{\Omega_l} L'_l$ 

```

Train the feedforward and feedback networks:

```

for  $i = 1$  to  $N$  do
  for all  $(x, y) \in D$  do
     $h_0 = x$ 
    for  $l = 1$  to  $L$  do
       $h_l = f_l(h_{l-1})$ 
    Update the feedback weights:
    for  $j = 1$  to  $N_b$  do
      for  $l = 1$  to  $L$  do
         $r_l = h_l + \epsilon$ ,  $\epsilon \sim N(0, \sigma I)$ 
         $r_{l+1} = f_{l+1}(r_l)$ 
         $r_l^{rec} = g_{l+1}(r_{l+1})$ 
         $L'_l = \|r_l^{rec} - r_l\|_2^2$ 
         $\Omega_l \leftarrow \Omega_l - \alpha_b \nabla_{\Omega_l} L'_l$ 
    Compute targets:
     $\tau_L = h_L - \beta \nabla_{h_L} \mathcal{L}(h_L, y)$ 
    for  $l = L - 1$  to  $1$  do
       $\tau_l = g_{l+1}(\tau_{l+1}) + h_l - g_{l+1}(h_{l+1})$ 
    Update the forward weights:
    for  $l = 1$  to  $L$  do
       $L_l = \|\tau_l - h_l\|_2^2$ 
       $W_l \leftarrow W_l - \alpha_f \nabla_{W_l} L_l$ 

```

- For Fashion-MNIST: 5 fully connected layers with 164 hidden units + 1 output softmax layer with 10 units.
- For CIFAR-10: 3 fully connected layers with 632 hidden units + 1 output softmax layer with 10 units.
- For CIFAR-100: 3 fully connected layers with 631 hidden units + 1 output softmax layer with 100 units.

Hyperparameters. We report the search sets of hyperparameters used in 4.2. Table 8 shows the search sets of the

Algorithm 3: DTP with Difference Reconstruction Loss (DRL) (Meulemans et al. 2020).

Hyperparameters: Learning Rate α_f , α_b , Stepsize β , Feedback Update Frequency N_b , Standard Deviation σ , Tikhonov damping constant λ

Requires: Dataset D , Loss \mathcal{L} , Epochs N , Encoder f_l parameterized with W_l ($l = 1 \dots L$), Decoder g_l parameterized with Ω_l ($l = 1 \dots L$)

Pre-train only feedback network:

```

for all  $(x, y) \in D$  do
   $h_0 = x$ 
  for  $l = 1$  to  $L$  do
     $h_l = f_l(h_{l-1})$ 
  Update the feedback weights:
  for  $j = 1$  to  $N_b$  do
    for  $l = 1$  to  $L$  do
       $r_l = h_l + \epsilon$ ,  $\epsilon \sim N(0, \sigma I)$ 
      for  $k = l + 1$  to  $L$  do
         $r_k = f_k(r_{k-1})$ 
       $r_L^{rec} = r_L$ 
      for  $k = L - 1$  to  $l$  do
         $r_k^{rec} = g_{k+1}(r_{k+1}^{rec}) + h_k - g_{k+1}(h_{k+1})$ 
       $L'_l = \|r_l^{rec} - r_l\|_2^2 + \lambda \|\Omega_l\|_F^2$ 
       $\Omega_l \leftarrow \Omega_l - \alpha_b \nabla_{\Omega_l} L'_l$ 

```

Train the feedforward and feedback networks:

```

for  $i = 1$  to  $N$  do
  for all  $(x, y) \in D$  do
     $h_0 = x$ 
    for  $l = 1$  to  $L$  do
       $h_l = f_l(h_{l-1})$ 
    Update the feedback weights:
    for  $j = 1$  to  $N_b$  do
      for  $l = 1$  to  $L$  do
         $r_l = h_l + \epsilon$ ,  $\epsilon \sim N(0, \sigma I)$ 
        for  $k = l + 1$  to  $L$  do
           $r_k = f_k(r_{k-1})$ 
         $r_L^{rec} = r_L$ 
        for  $k = L - 1$  to  $l$  do
           $r_k^{rec} = g_{k+1}(r_{k+1}^{rec}) + h_k - g_{k+1}(h_{k+1})$ 
         $L'_l = \|r_l^{rec} - r_l\|_2^2 + \lambda \|\Omega_l\|_F^2$ 
         $\Omega_l \leftarrow \Omega_l - \alpha_b \nabla_{\Omega_l} L'_l$ 
      Compute targets:
       $\tau_L = h_L - \beta \nabla_{h_L} \mathcal{L}(h_L, y)$ 
      for  $l = L - 1$  to  $1$  do
         $\tau_l = g_{l+1}(\tau_{l+1}) + h_l - g_{l+1}(h_{l+1})$ 
      Update the forward weights:
      for  $l = 1$  to  $L$  do
         $L_l = \|\tau_l - h_l\|_2^2$ 
         $W_l \leftarrow W_l - \alpha_f \nabla_{W_l} L_l$ 

```

learning rate for the feedforward network α_f , the stepsize β and the learning rate for the feedback network α_b for DTP,

Algorithm 4: DTP with Local Difference Reconstruction Loss (L-DRL) (Ernout et al. 2022).

Hyperparameters: Learning Rate α_f , α_b , Stepsize β , Feedback Update Frequency N_b , Standard Deviation σ

Requires: Dataset D , Loss \mathcal{L} , Epochs N , Encoder f_l parameterized with W_l ($l = 1 \dots L$), Decoder g_l parameterized with Ω_l ($l = 1 \dots L$)

Pre-train only feedback network:

```

for all  $(x, y) \in D$  do
   $h_0 = x$ 
  for  $l = 1$  to  $L$  do
     $h_l = f_l(h_{l-1})$ 
  Update the feedback weights:
  for  $j = 1$  to  $N_b$  do
    for  $l = 1$  to  $L$  do
       $r_l = h_l + \epsilon$ ,  $\epsilon \sim N(0, \sigma I)$ 
       $r_{l+1} = f_{l+1}(r_l)$ 
       $r_l^{rec} = g_{l+1}(r_{l+1}) + h_l - g_{l+1}(h_l)$ 
       $s_{l+1} = h_{l+1} + \eta$ ,  $\eta \sim N(0, \sigma I)$ 
       $s_l^{rec} = g_{l+1}(s_{l+1}) + h_l - g_{l+1}(h_l)$ 
       $L'_l =$ 
         $-(r_l - h_l)^t (r_l^{rec} - h_l) + \frac{1}{2} \|s_l^{rec} - h_l\|_2^2$ 
       $\Omega_l \leftarrow \Omega_l - \alpha_b \nabla_{\Omega_l} L'_l$ 

```

Train the feedforward and feedback networks:

```

for  $i = 1$  to  $N$  do
  for all  $(x, y) \in D$  do
    Propagate activations:
     $h_0 = x$ 
    for  $l = 1$  to  $L$  do
       $h_l = f_l(h_{l-1})$ 
    Update the feedback weights:
    for  $j = 1$  to  $N_b$  do
      for  $l = 1$  to  $L$  do
         $r_l = h_l + \epsilon$ ,  $\epsilon \sim N(0, \sigma I)$ 
         $r_{l+1} = f_{l+1}(r_l)$ 
         $r_l^{rec} = g_{l+1}(r_{l+1}) + h_l - g_{l+1}(h_l)$ 
         $s_{l+1} = h_{l+1} + \eta$ ,  $\eta \sim N(0, \sigma I)$ 
         $s_l^{rec} = g_{l+1}(s_{l+1}) + h_l - g_{l+1}(h_l)$ 
         $L'_l =$ 
           $-(r_l - h_l)^t (r_l^{rec} - h_l) + \frac{1}{2} \|s_l^{rec} - h_l\|_2^2$ 
         $\Omega_l \leftarrow \Omega_l - \alpha_b \nabla_{\Omega_l} L'_l$ 
      Compute targets:
       $\tau_L = h_L - \beta \nabla_{h_L} \mathcal{L}(h_L, y)$ 
      for  $l = L - 1$  to  $1$  do
         $\tau_l = g_{l+1}(\tau_{l+1}) + h_l - g_{l+1}(h_{l+1})$ 
      Update the forward weights:
      for  $l = 1$  to  $L$  do
         $L_l = \|\tau_l - h_l\|_2^2$ 
         $W_l \leftarrow W_l - \alpha_f \nabla_{W_l} L_l$ 

```

DRL and L-DRL. These search sets were determined by a rough tuning of 10-fold intervals and used for all datasets. The feedback update frequency N_b , standard deviation σ and

Table 8: Search sets of hyperparameters of DTP, DRL and L-DRL for all datasets.

HYPERPARAMETER	SEARCH SET
LEARNING RATE α_f	{0.1, 0.2, 0.4, 0.8, 1, 2, 4, 8}
STEP SIZE β	{0.001, 0.002, 0.004, 0.008, 0.01, 0.02, 0.04, 0.08}
LEARNING RATE α_b	{0.0001, 0.0002, 0.0004, 0.0008, 0.001, 0.002, 0.004, 0.008}

Table 9: Search sets of hyperparameters of FW-DTP for MNIST and F-MNIST.

HYPERPARAMETER	SEARCH SET
LEARNING RATE α_f	{0.1, 0.2, 0.4, 0.8, 1, 2, 4, 8}
STEP SIZE β	{0.001, 0.002, 0.004, 0.008, 0.01, 0.02, 0.04, 0.08}

Table 10: Search sets of hyperparameters of FW-DTP for CIFAR-10/100.

HYPERPARAMETER	SEARCH SET
LEARNING RATE α_f	{0.01, 0.02, 0.04, 0.08, 0.1, 0.2, 0.4, 0.8}
STEP SIZE β	{0.001, 0.002, 0.004, 0.008, 0.01, 0.02, 0.04, 0.08}

Table 11: The best hyperparameters used in 4.1 and 4.2.

DATASET	HYPERPARAMETER	DTP	DRL	L-DRL	FW-DTP
MNIST	LEARNING RATE α_f	4	4	4	0.1
	STEP SIZE β	0.04	0.04	0.04	0.04
	LEARNING RATE α_b	0.002	0.0002	0.0002	–
F-MNIST	LEARNING RATE α_f	1	4	2	1
	STEP SIZE β	0.04	0.008	0.02	0.004
	LEARNING RATE α_b	0.002	0.002	0.001	–
CIFAR-10	LEARNING RATE α_f	4	2	0.2	0.02
	STEP SIZE β	0.002	0.008	0.04	0.01
	LEARNING RATE α_b	0.004	0.004	0.0004	–
CIFAR-100	LEARNING RATE α_f	1	0.8	2	0.2
	STEP SIZE β	0.01	0.02	0.008	0.01
	LEARNING RATE α_b	0.008	0.002	0.0001	–

batch size M were fixed to reduce tuning costs, and we used $N_b = 5$, $\sigma = 0.01$ and $M = 256$. Note that, while the learning rates are sensitive to choice, the standard deviation had little effect on learning even when the value was set to 10x or 0.1x. For DRL, the Tikhonov damping constant λ was also fixed to 0, *i.e.*, no regularization was applied. For FW-DTP, the search sets of the learning rate for the feedforward network α_f and the stepsize β used for MNIST and F-MNIST are shown in Table. 9. These search sets are same as those of DTP, but for CIFAR10/100, a different search sets were obtained as a result of the abovementioned rough tuning and shown in Figure 10.

For DTP, DRL and L-DRL, we initialized the weights of the feedforward networks with orthogonal matrices for all datasets. For FW-DTP, we also used orthogonal matrices to initialize the weights of the feedforward network; however,

the weights of the feedback network were initialized with a uniform distribution $U(-10^{-2}, 10^{-2})$.

The best hyperparameters used in 4.2 are shown in Table 11. These best hyperparameters were also used in 4.1. To find these best hyperparameters, grid search was used; 5000 samples from training set were used as a validation set, and the set of hyperparameters which obtained the best test performance at 100 epoch were chosen as the best hyperparameters.

Hyperparameter Sampling in Sec. 4.3. Tables 12 and 13 show sampled hyperparameters used in the evaluation of hyperparameter sensitivity in Section 4.3. The number of hyperparameters H is three for DTP and two for FW-DTP. Note that for a fair comparison, each hyperparameter γ was randomly sampled so that $\log(\gamma) \sim U(\log(0.2\tilde{\gamma}), \log(5\tilde{\gamma}))$ where U is the uniform distribution and $\tilde{\gamma}$ is the best hy-

Table 12: Search spaces of hyperparameters used in 4.3 for DTP.

HYPERPARAMETER	BEST $\bar{\gamma}$	SEARCH SPACE $[0.2\bar{\gamma}, 5\bar{\gamma}]$
LEARNING RATE α_f	4	$[0.8, 20]$
STEP SIZE β	0.002	$[0.0004, 0.01]$
LEARNING RATE α_b	0.004	$[0.0008, 0.02]$

Table 13: Search spaces of hyperparameters used in 4.3 for FW-DTP.

HYPERPARAMETER	BEST $\bar{\gamma}$	SEARCH SPACE $[0.2\bar{\gamma}, 5\bar{\gamma}]$
LEARNING RATE α_f	0.02	$[0.004, 0.1]$
STEP SIZE β	0.01	$[0.002, 0.05]$

perparameter used in Section 4.2. The best hyperparameter used in 4.2 and the range $[0.2\bar{\gamma}, 5\bar{\gamma}]$ is shown in the table.